INTERACTION OF HIGH INTENSITY LASER WITH STRUCTURED SNOW TARGETS

A.Zigler
Hebrew University of Jerusalem
Israel
and
INFN Frascati Italy

IZEST 2015
CERN , Switzerland

Collaborators :

Z.Henis, M. Botton, S. Eisenman, E. Schleifer

Hebrew Univ. Jerusalem

D. Gordon, P. Sprangle **NRL Washington DC**

R. Pompili, M.P. Anania FLAME LASER INFN

F. G Bisesto M. Galletti Frascatti Italy

Proton energy vs. laser power (current status)

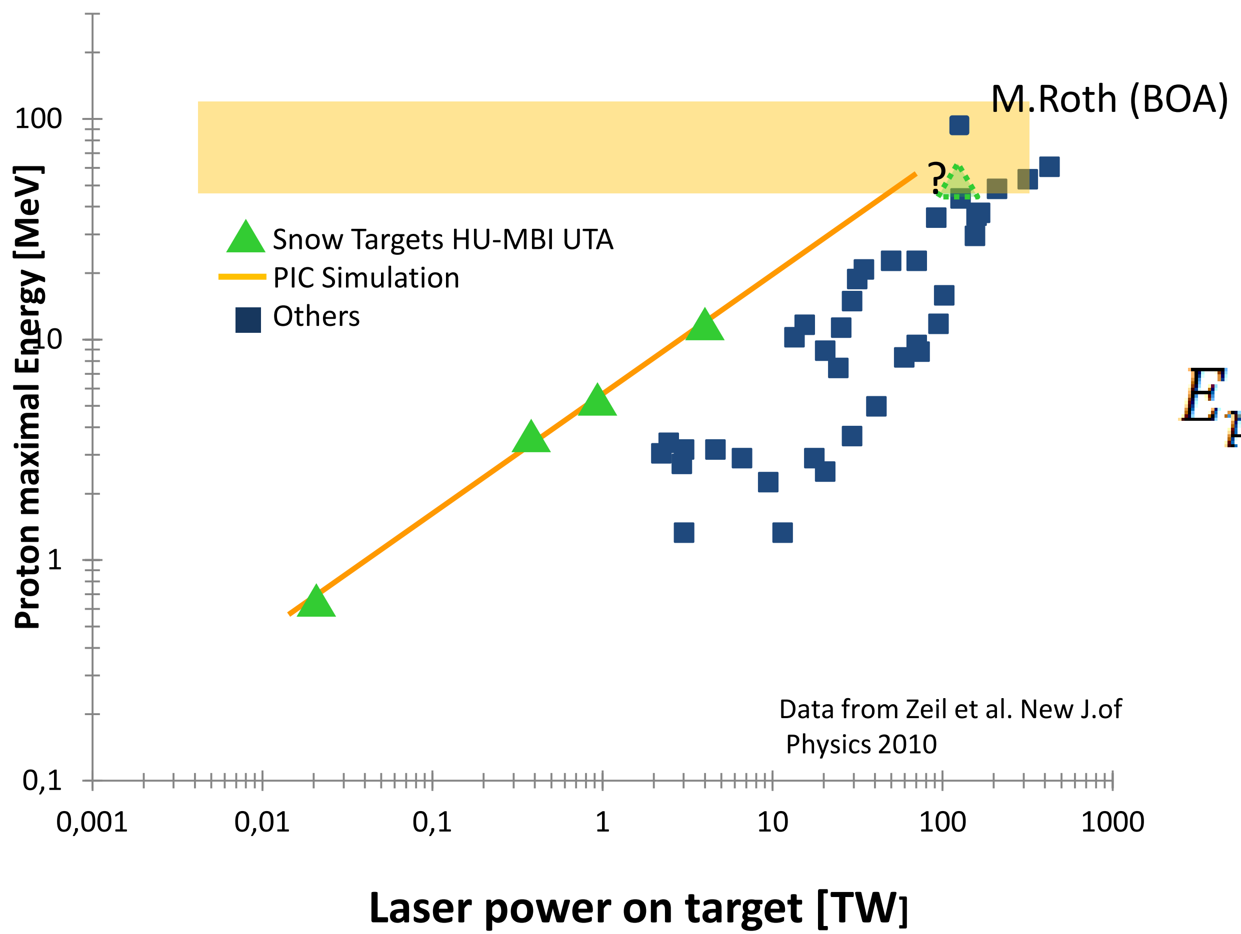

$$E_p \sim P_L^{1/2}$$

Enhanced proton acceleration from snow (microwire) targets

The higher proton energy can be attributed to several effects:

- **The density gradient generated by the laser prepulse.**
- **Mass limited phenomenon.**
- **Localized field enhancement by the local plasma density near the tip of snow needle.**
- **Coulomb explosion of the positively charged snow needle, adding longtime acceleration of the protons.**
- **Aspect ratio of the microwire.**

Highly structured snow surface

The snow is growing as pillars in the” normal” direction to the substrate.

The aspect ratio of the pillars decreases as the scale size decreases. The smallest features, spatially resolved, are with diameter about 0.5 - 2 μm

The surface can be characterized by three roughness scales:

a) pillars of about 100 μm

b) spikes of about 10 μm on top of them

c) whiskers of about 1 μm on the spikes.

Control of the structured snow target by changing the flow rate and varying the nucleation centers

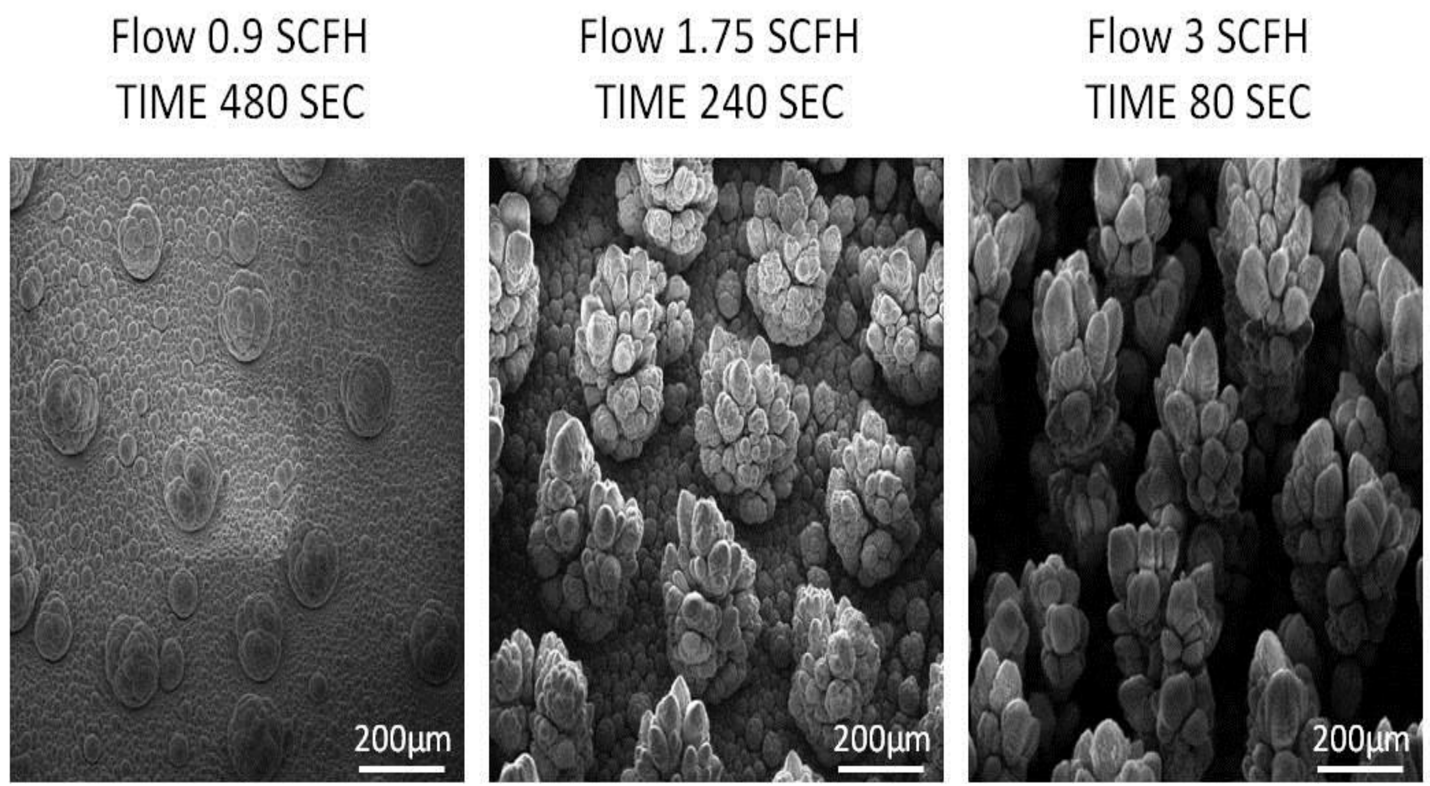

SEM images of snow pillars that were grown over artificial Aluminum nucleation centers on Sapphire substrate at various growth conditions.

Control of morphology by growth kinetics

0.9 SCFH, 480 sec

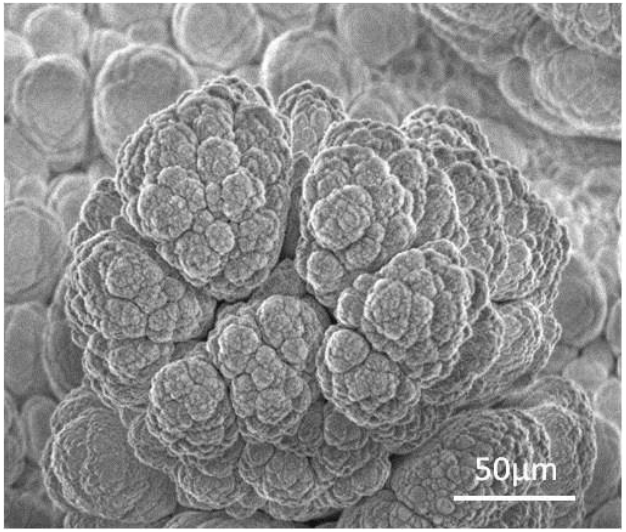

3 SCFH, 80 sec

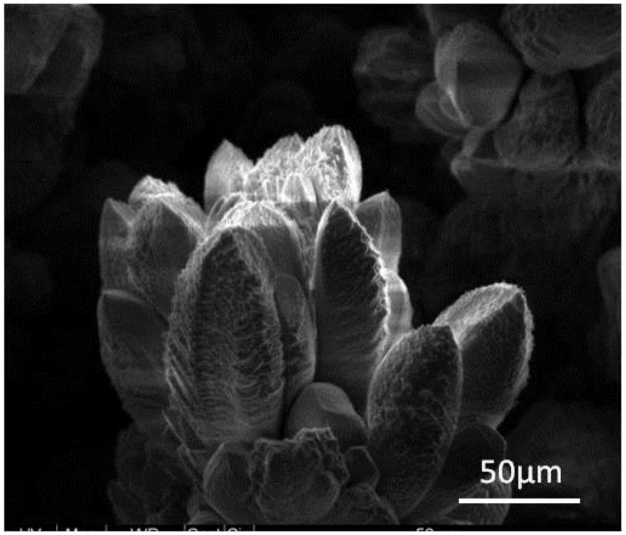

Influence of the pre pulse

(damage threshold of the snow target

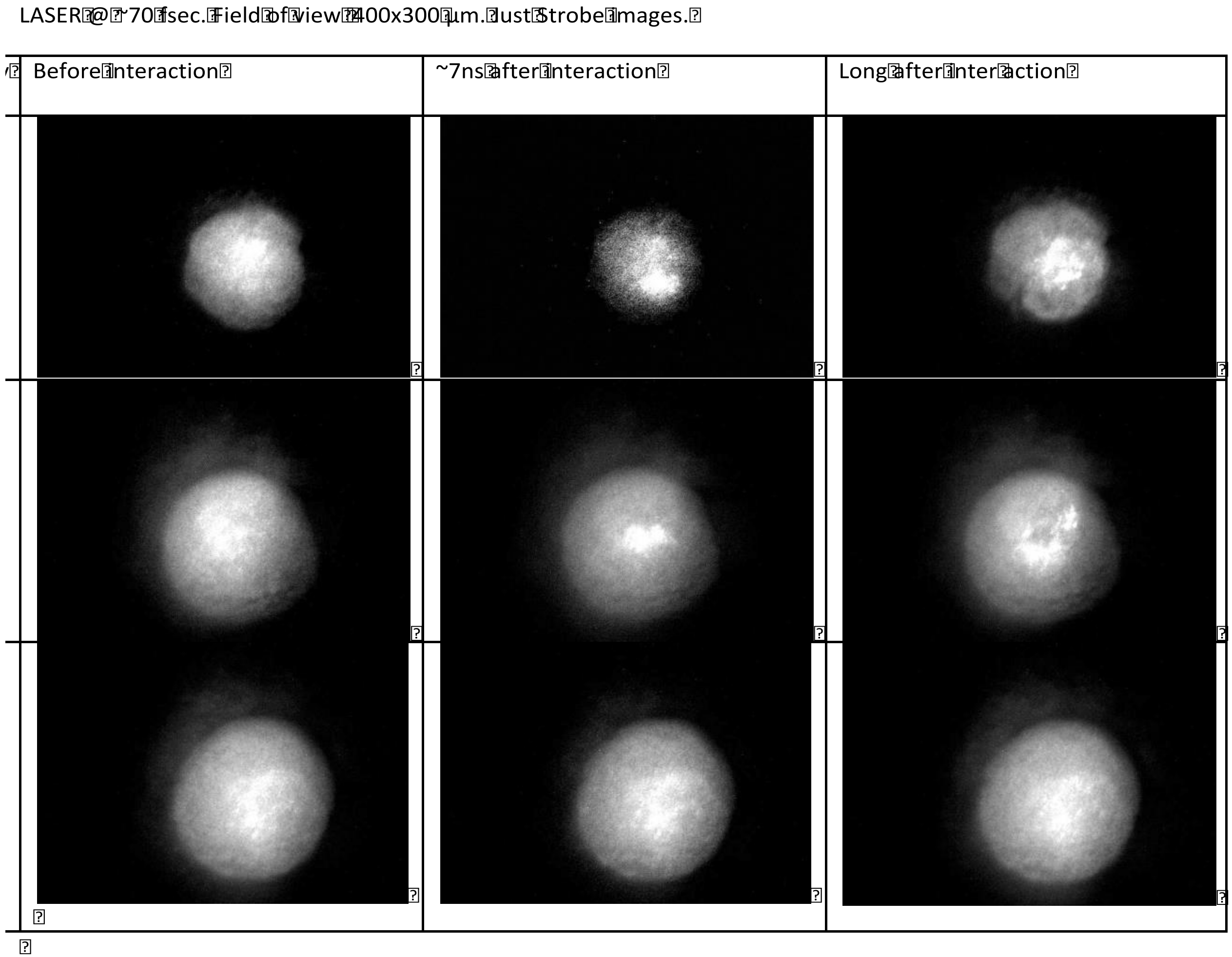

96µj

26µj

10µj

The damage threshold – 0.3j/cm^2

Less than 1 microjoule for tight (<10 micron) focusing !

Experimental Setup

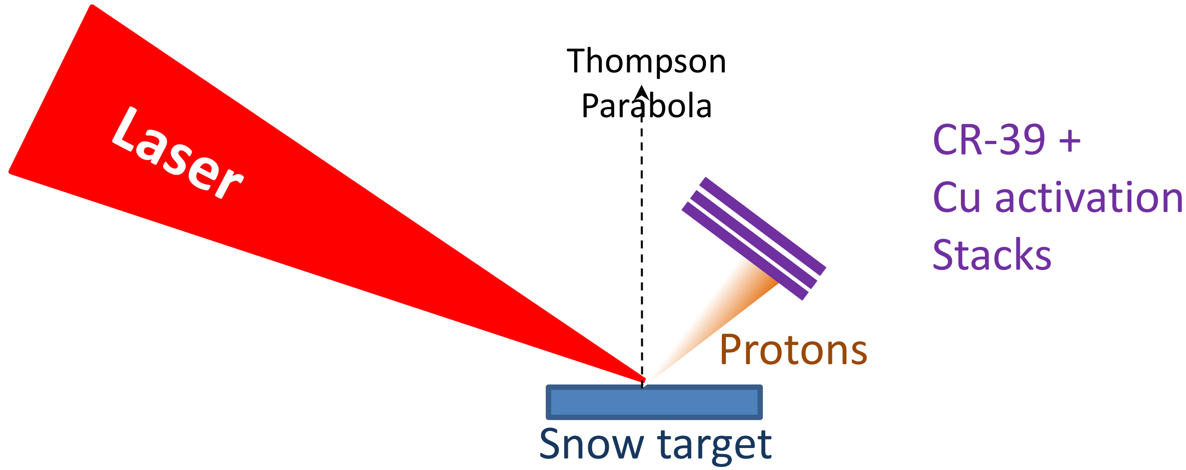

Laser Parameters	HU	MBI (up to 10TW on target in or exper.)	Texas PTW (40TW on target in our experiment)
Energy (on target)	50 mJ	400 mJ	100 J
Pulse Duration	50 fsec	65 fsec	150fsec
Spot Size	10 um^2	10 um^2	10 um^2 (multi spots)
Contrast Ratio	10^{-4} (10 nsec)	10^{-5} (6 nsec) (artificial pre-pulse)	10^{-6} (100 nsec ,many prepulses) 10^{-8} (with plasma mirror)

Max Proton Energy vs. Intensity

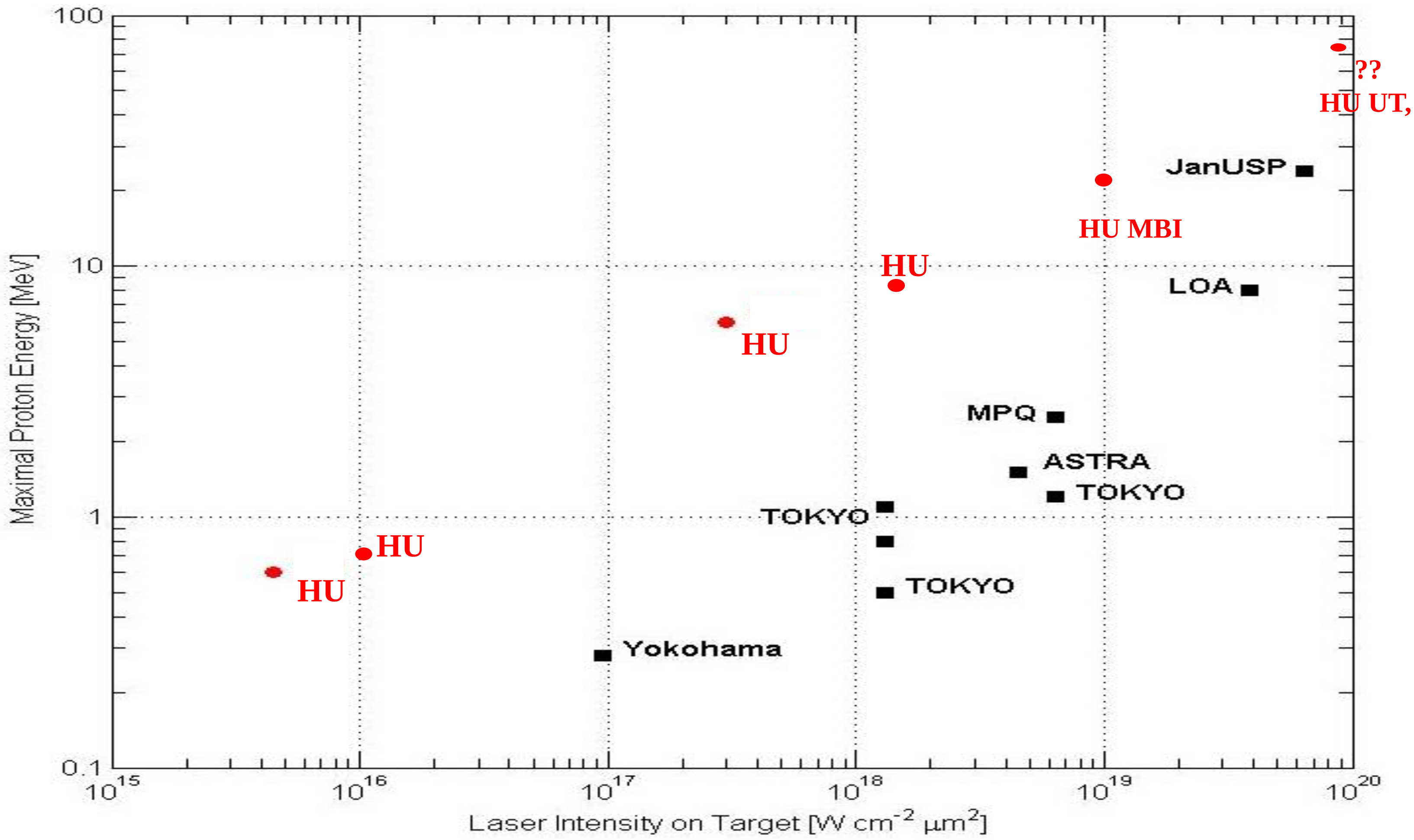

What is a possible origin of these higher energies? We need modeling.

Model of laser whisker interaction

- Interaction of the laser with a single wire.
- Use the prepulse with the same time duration as the main pulse - generates plasma with temperature of 2–5 eV.
- During the 10 ns interval between the prepulse and the main pulse the plasma expands forming a cylindrical plasma column.
- The main pulse interacts with a proper density scale length plasma.

Laser – snow wire interaction by 2D PIC simulations with TURBOWAVE

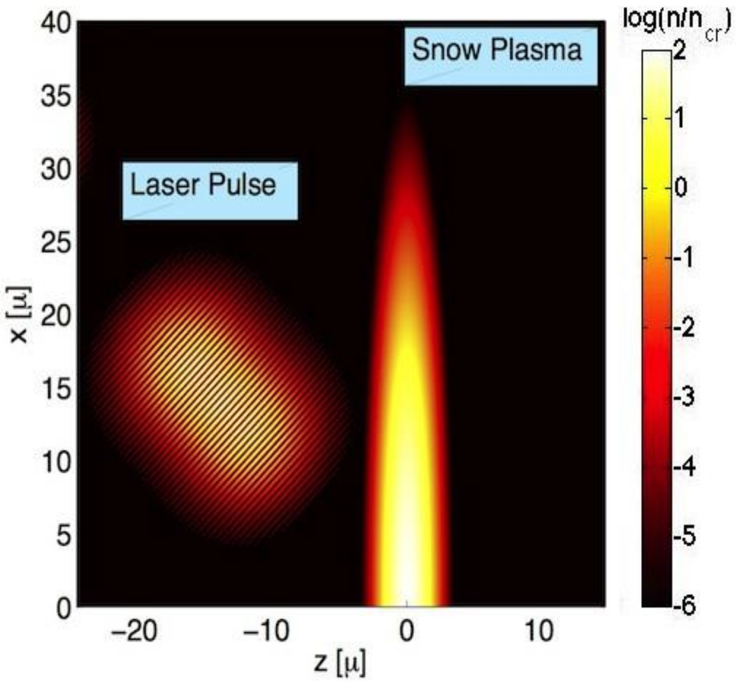

Laser: 88 fs (32 + 24 + 32), 0.8 μm, 4-5 μm spot size, $2.5 \cdot 10^{17} – 2.5 \cdot 10^{19}$ W/cm^2

The core of $100 \cdot n_{cr}$, : ellipsoid ~ 0.1-0.2μm x 1-2μm .
The critical density contour: ellipsoid ~ 1-2μm x 10μm .

TURBOWAVE, Gordon et al., IEEE Trans. Plasma Sci. 35, 1486 (2007).

Electrons

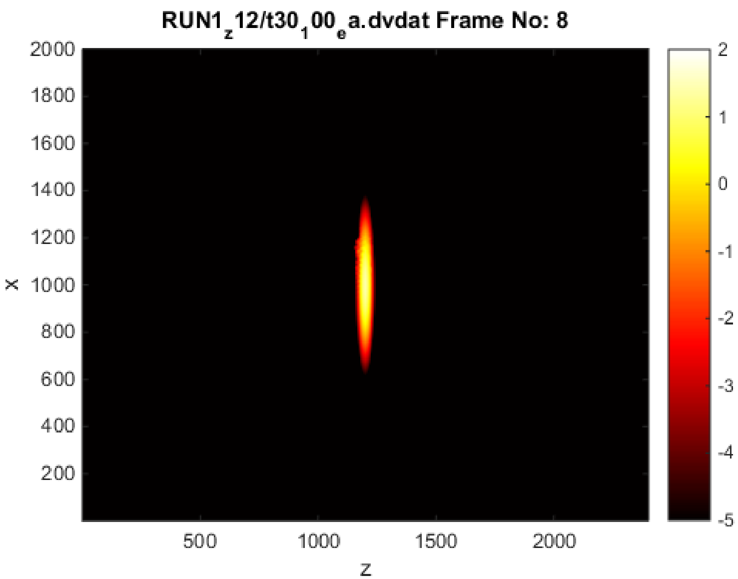

36 fs

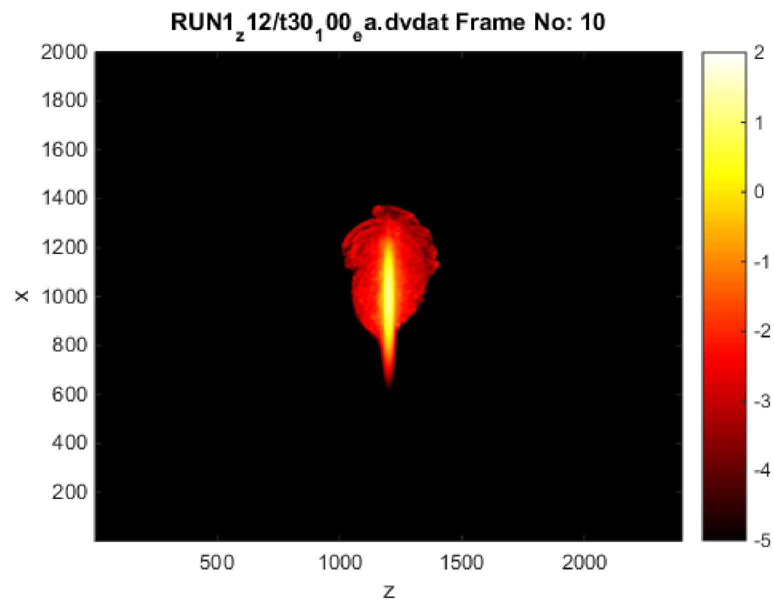

212 fs

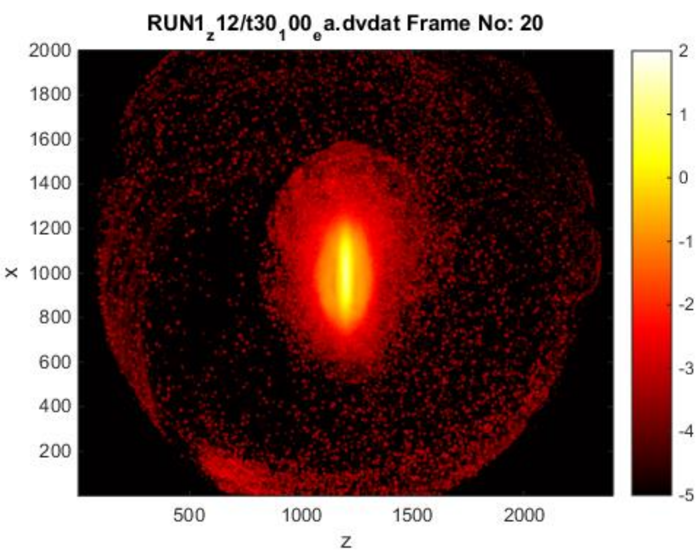

390 fs

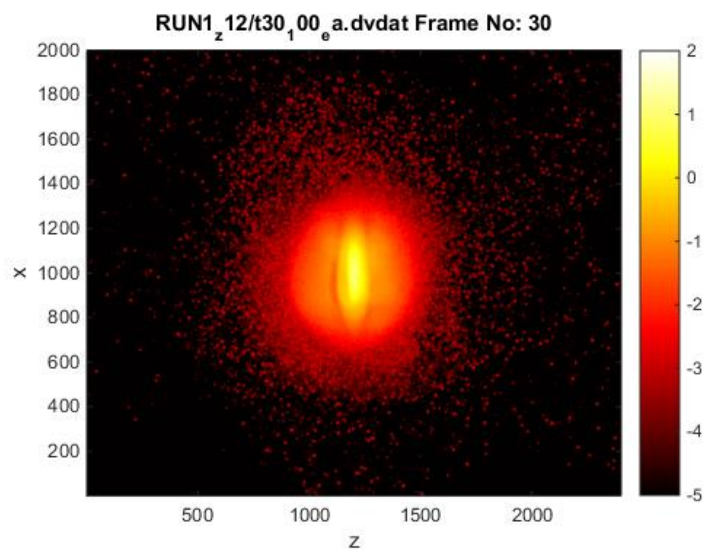

Protons

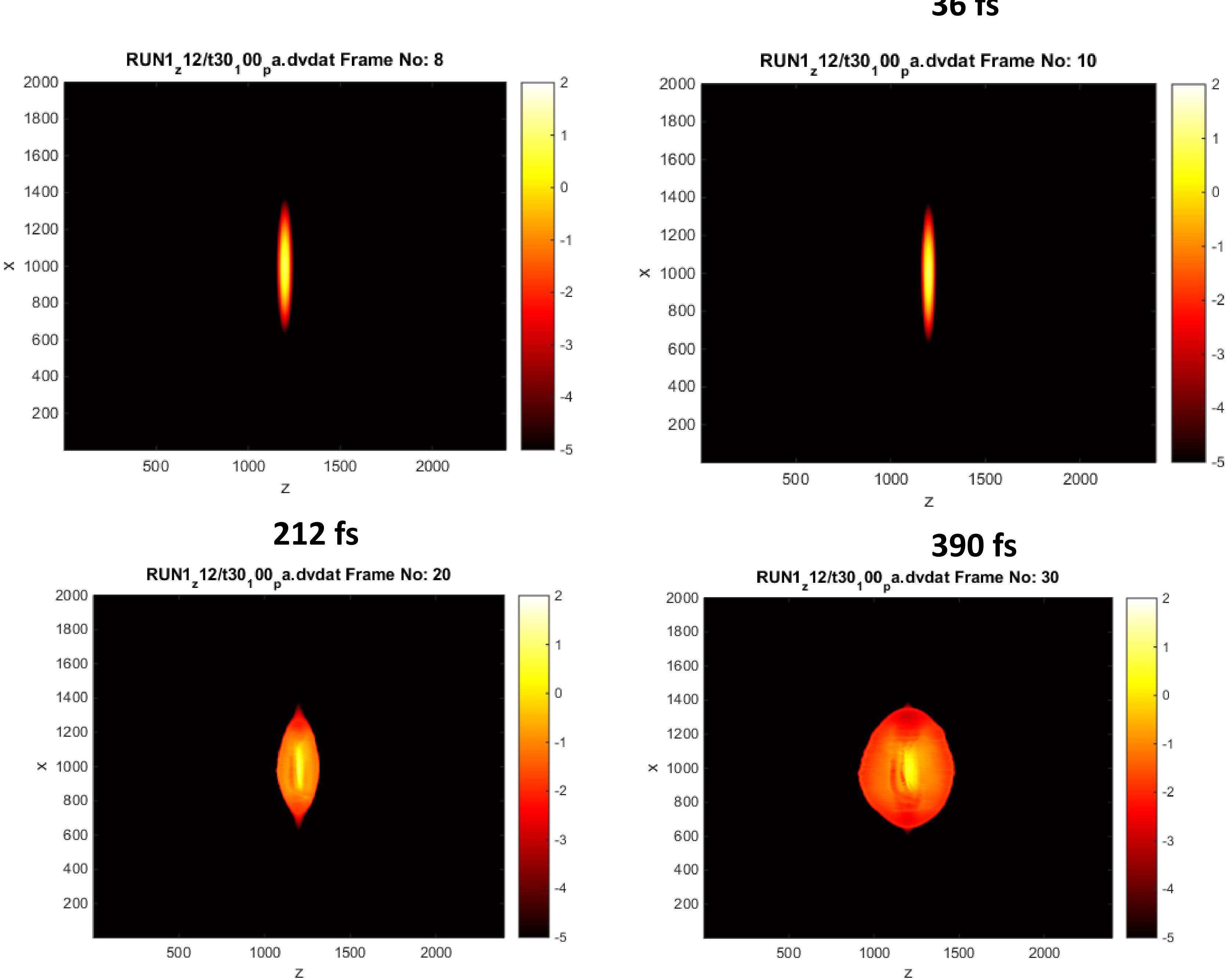
36 fs
RUN1_z12/t30_1 00_pa.dvdat Frame No: 8
RUN1_z12/t30_1 00_pa.dvdat Frame No: 10
212 fs
390 fs
RUN1_z12/t30_1 00_pa.dvdat Frame No: 20
RUN1_z12/t30_1 00_pa.dvdat Frame No: 30
x
z
2000
1800
1600
1400
1200
1000
800
600
400
200
500
1000
1500
2000
2
1
0
-1
-2
-3
-4
-5

The electric field in units of a_0

(x 1.37·10^{11} V/cm) I_L = 2.5·10^{19} W/cm^2

after 200fsec

$$a_0 = \frac{eE}{mc\omega}$$

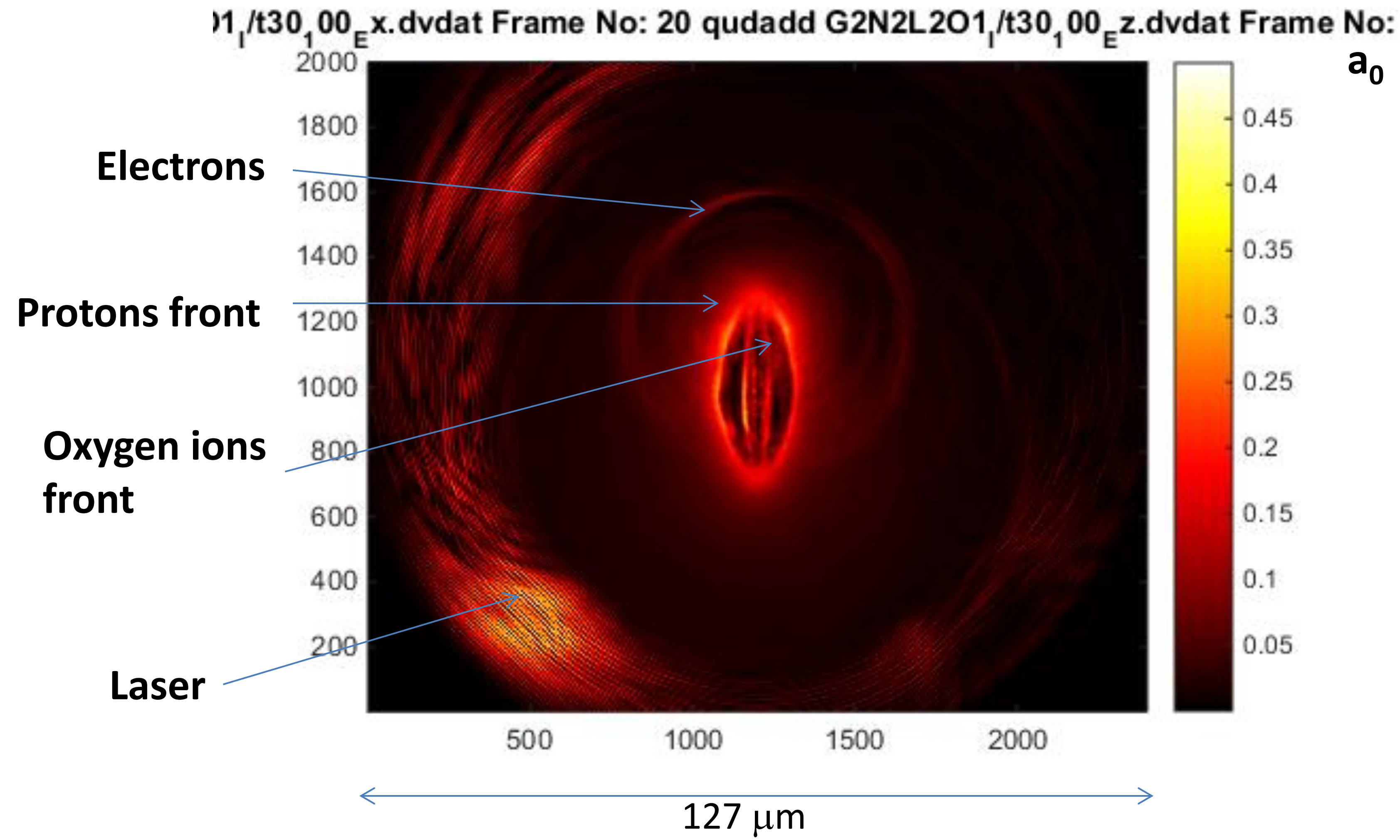

Constant solid density

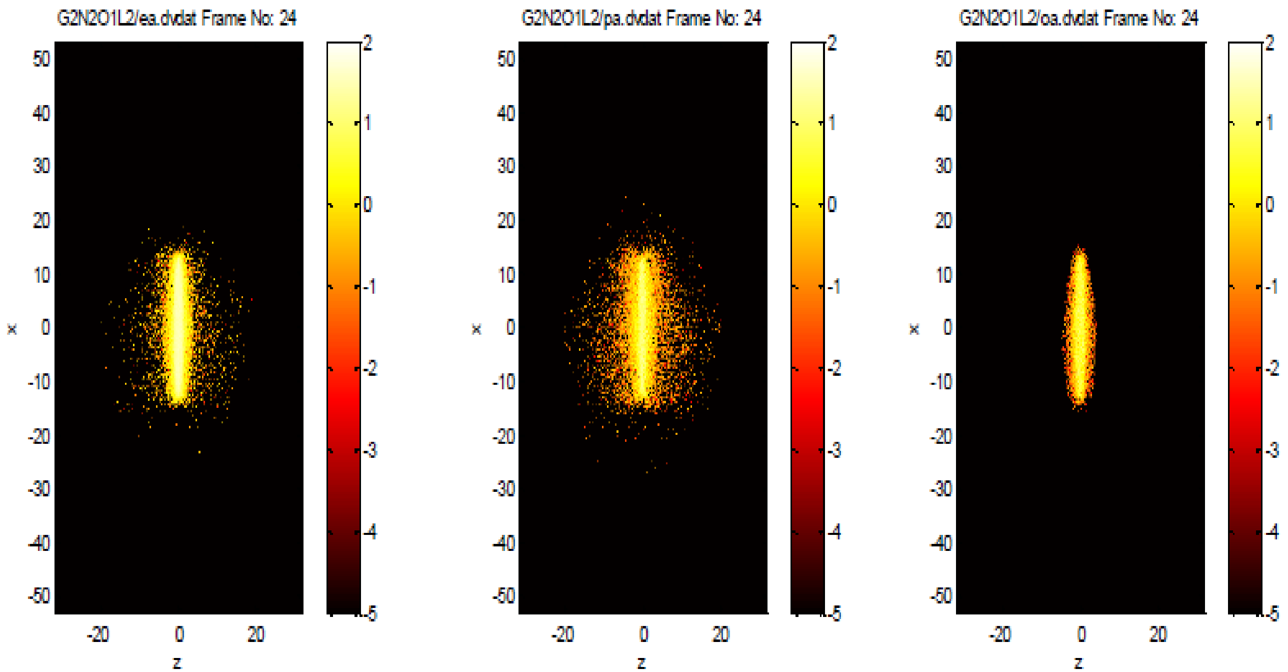

Electrons **Protons** **Oxygen**

I_L = 2.5·10^{19} W/cm^2, propagating at 45º relatively to the whisker major axis.
Time = 672 fs after the laser pulse hit the whiskers.

Acceleration process

- Electrons are driven out of the plasma ellipsoid, starting charge separation ~ τ_L . Unlike TNSA, no difference between front and rear surface.
- After passage of the laser, electrons accumulate near the tip, the protons start to react, ~ (2 -3) τ_L.
- The electrons accumulation near the tip is reduced, charge separation still maintained, (3 – 6) τ_L. Oxygen ions add a pushing field.
- Late times, acceleration ceases, the protons move at constant velocity.

Zigler et al. PRL 110, 2013.

Can we measure the temporal profile of an electrical field generated during the interaction of a high intensity laser pulse with a single wire?

- Possible approach –use of electro optical sampling

  Requirements:

1. 30 fs synchronization between the main (interacting) beam and the probe beam
2. Spatial overlap better than 30 microns

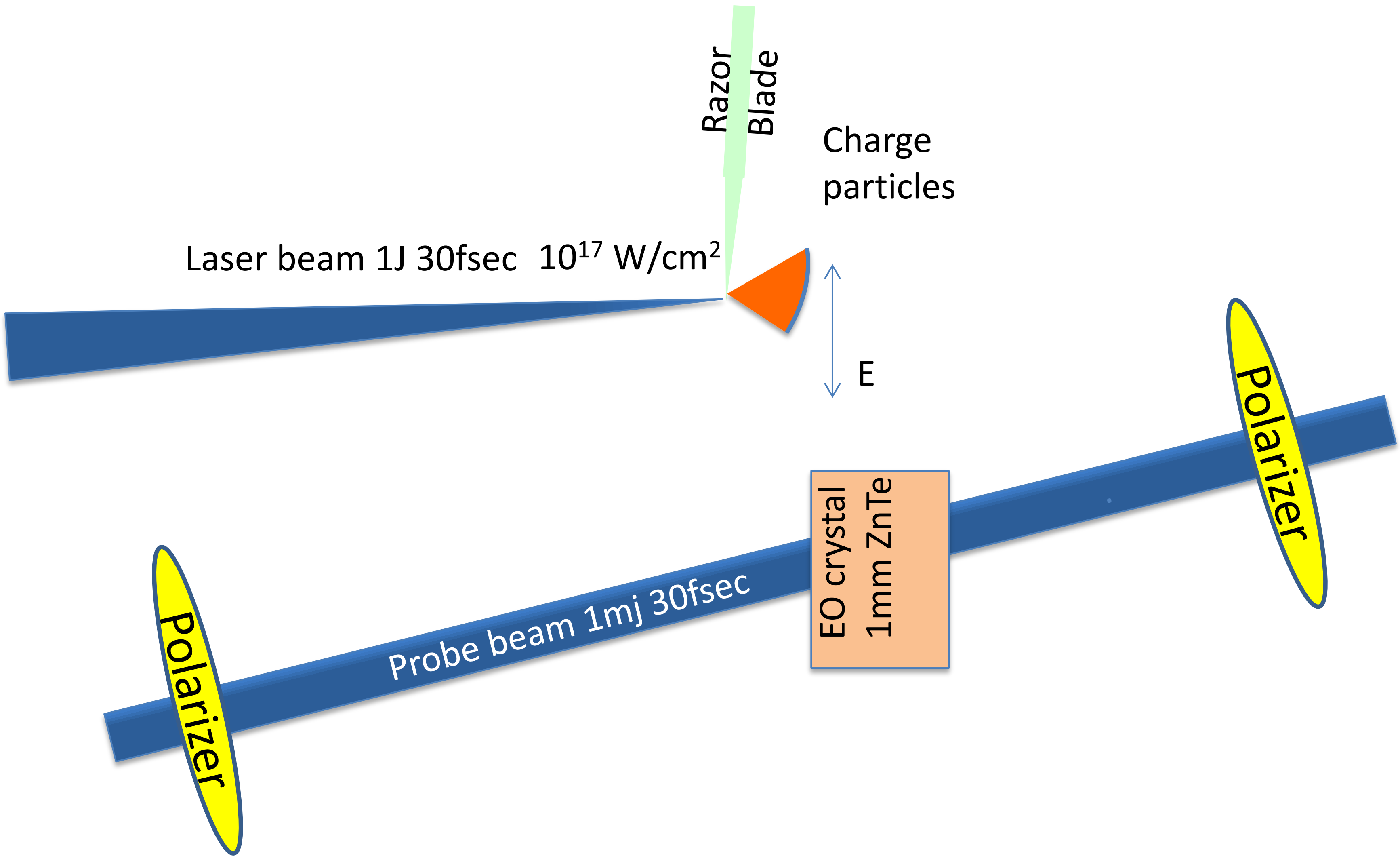

Electrical field measurement schematics – first steps

Electro-Optical Sampling

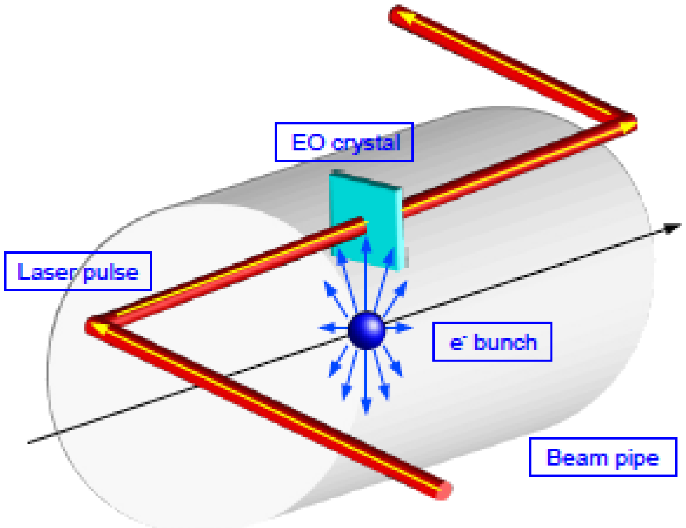

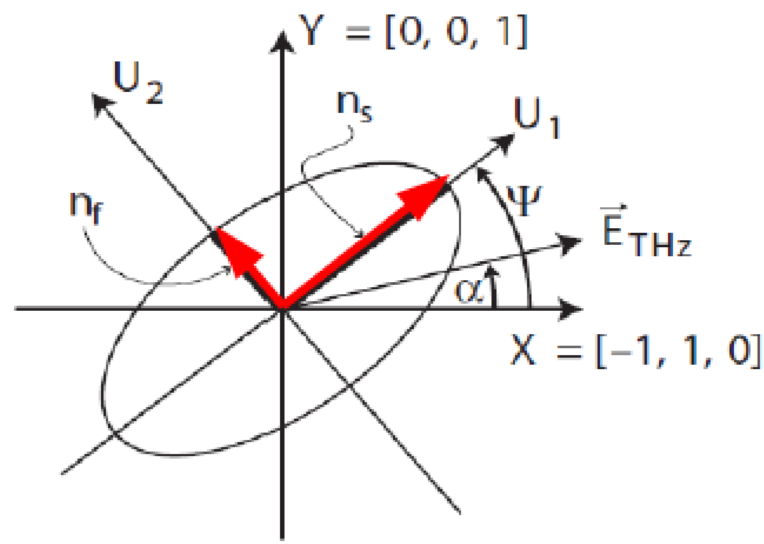

- Based on **Electro-Optic effect** in nonlinear crystals (**ZnTe, GaP**).
- The crystal becomes **anisotropic** → **2 different** refractive indices.
- Induced phase delay in a polarized laser propagating into it:

$$\Gamma(t) = \frac{\omega d}{c}(n_1 - n_2) = \frac{\omega d}{2c} n_0^3 r_{41} E_{THz}(t)\sqrt{1+3\cos^2\alpha}$$

- Benefits: <u>single shot</u>, <u>non-intercepting</u>, time resolution (50 fs rms)

Electrical Field due to Charged Particles Generated by Interaction of 10^{17} W/cm^2 40fsec Laser Beam with the Blade edge

(preliminary results)

7psec

Measured at 2mm from the blade edge

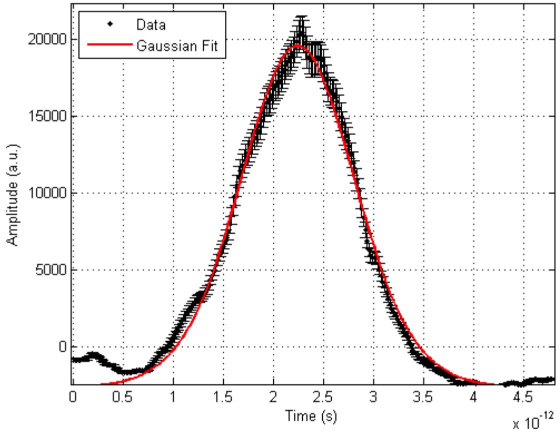

- **Electric Field: 7.5 MV/m**
- **Duration: 740 fs (rms)**

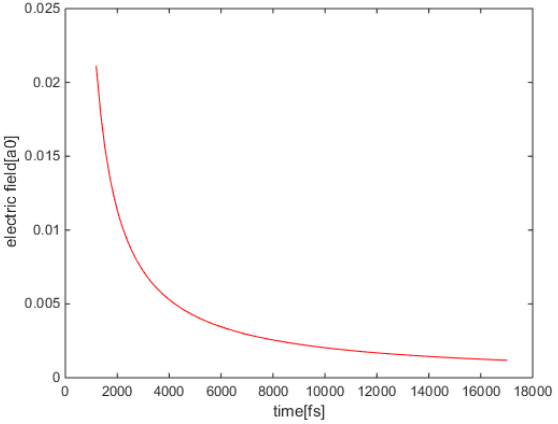

Summary: Proton energy vs. Laser power using micro- structured targets

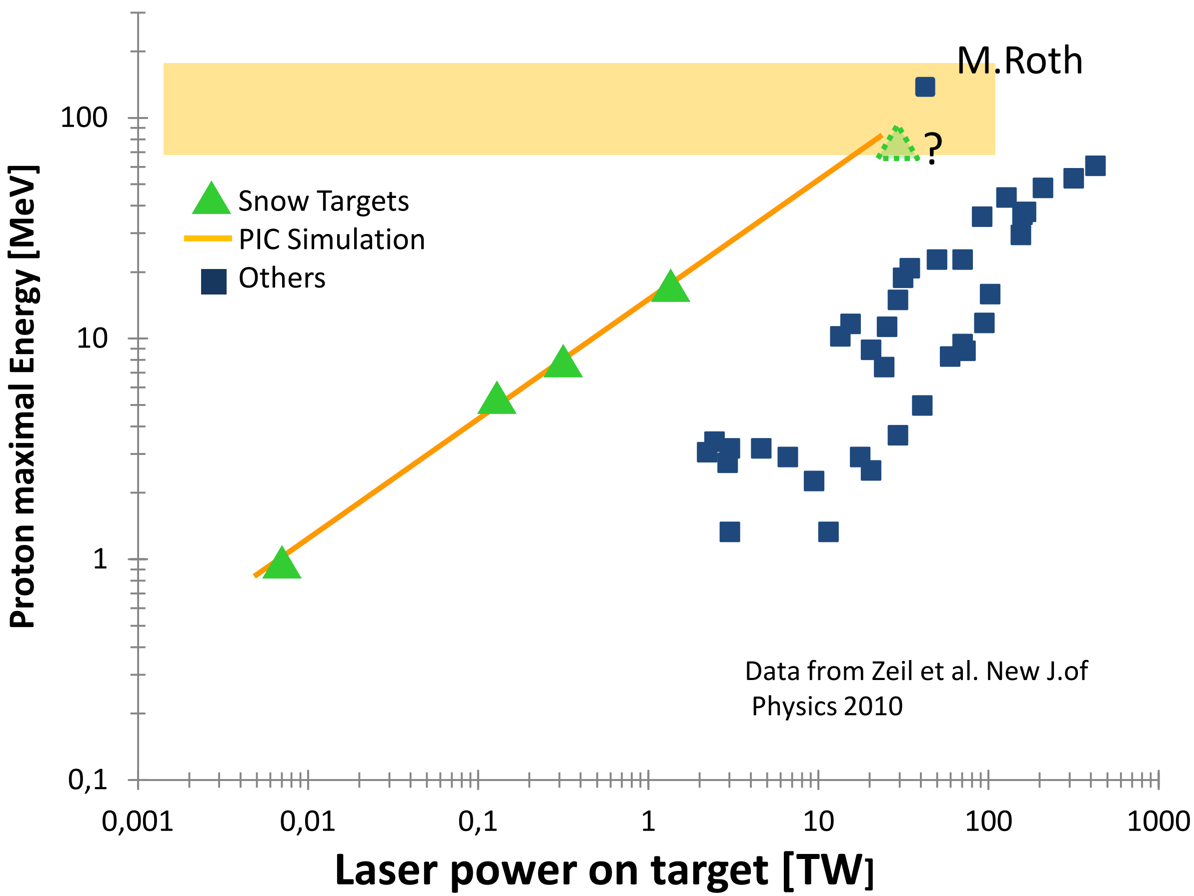

Thank you

EOS Spatial Encoding Setup

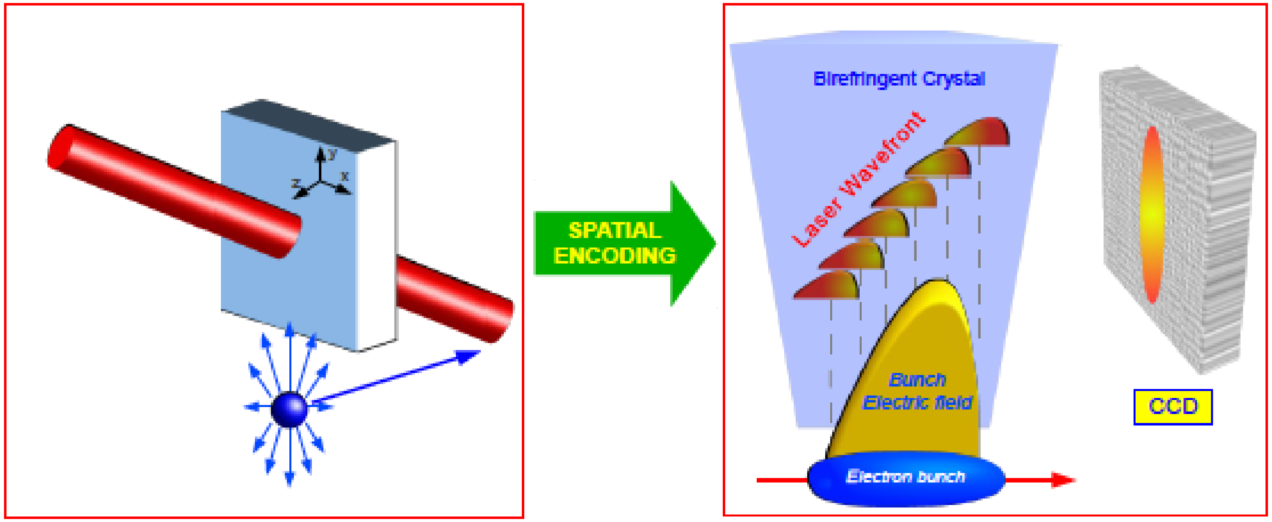

- Laser crosses the crystal with an incident angle of 30° → one side of the laser pulse arrives earlier on the EO crystal than the other by a time difference Δt.
- Coulomb field inducing birefringence is encoded in the spatial profile of laser pulse
- Benefits: **simple**, **no high energy laser needed**.
- Crossed Polarizer Setup
  - *Measured intensity is equal to* $I_{det} = I_{laser} \sin^2 \Gamma \propto E_{THz}^2$

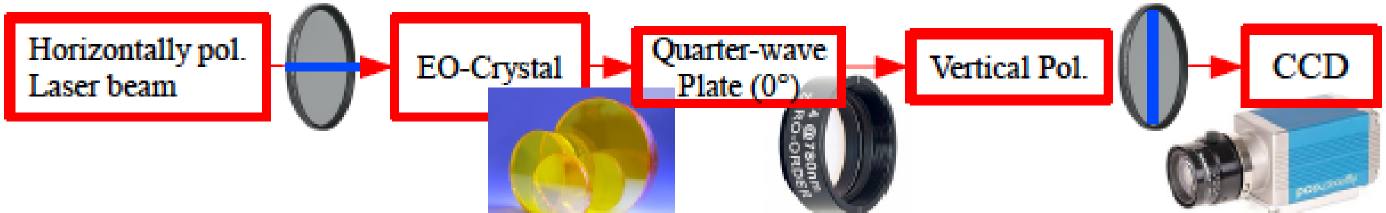

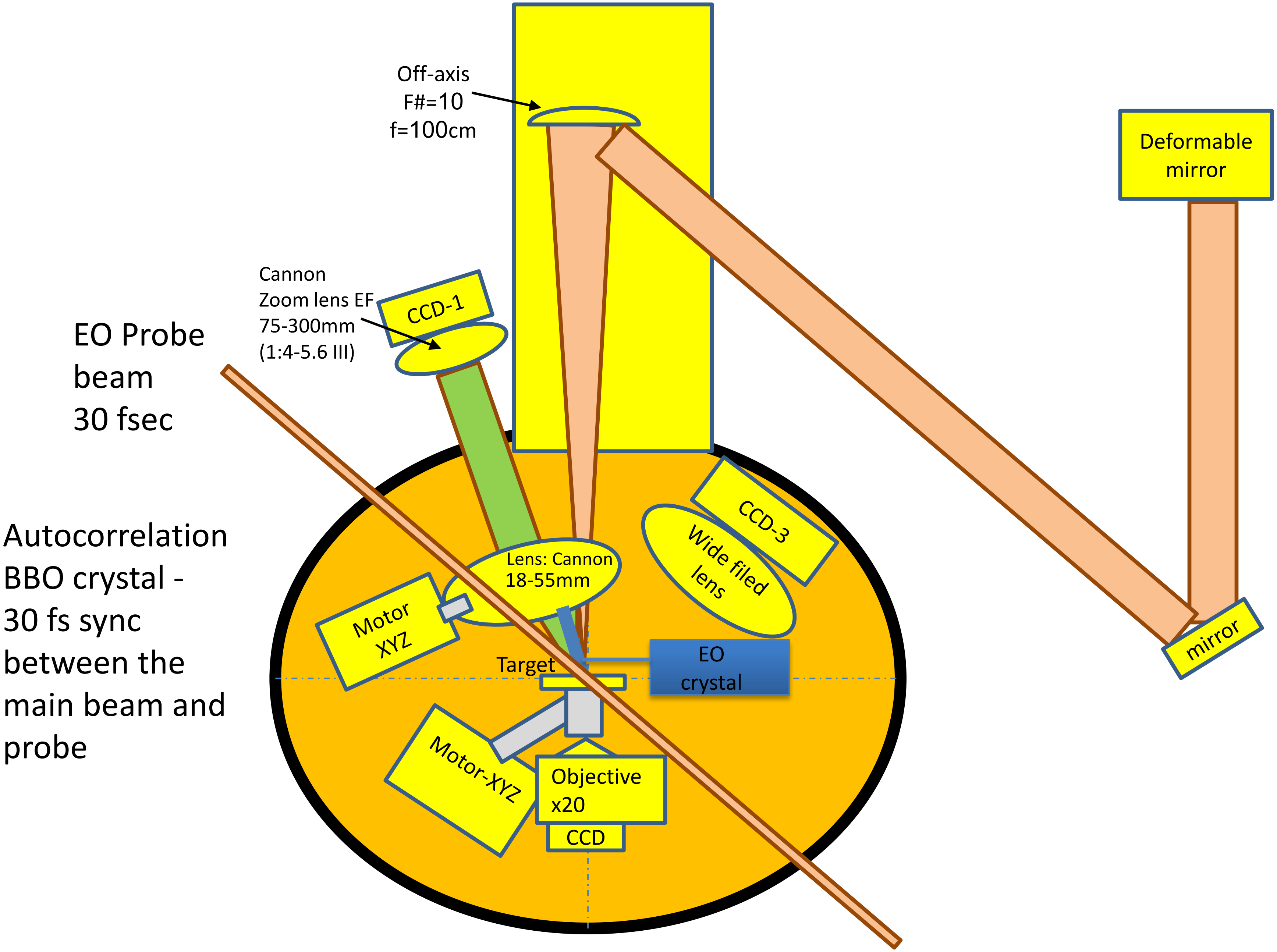

Experimental set up for electrical field measurement at FLAME laser

Snow target In the ESEM

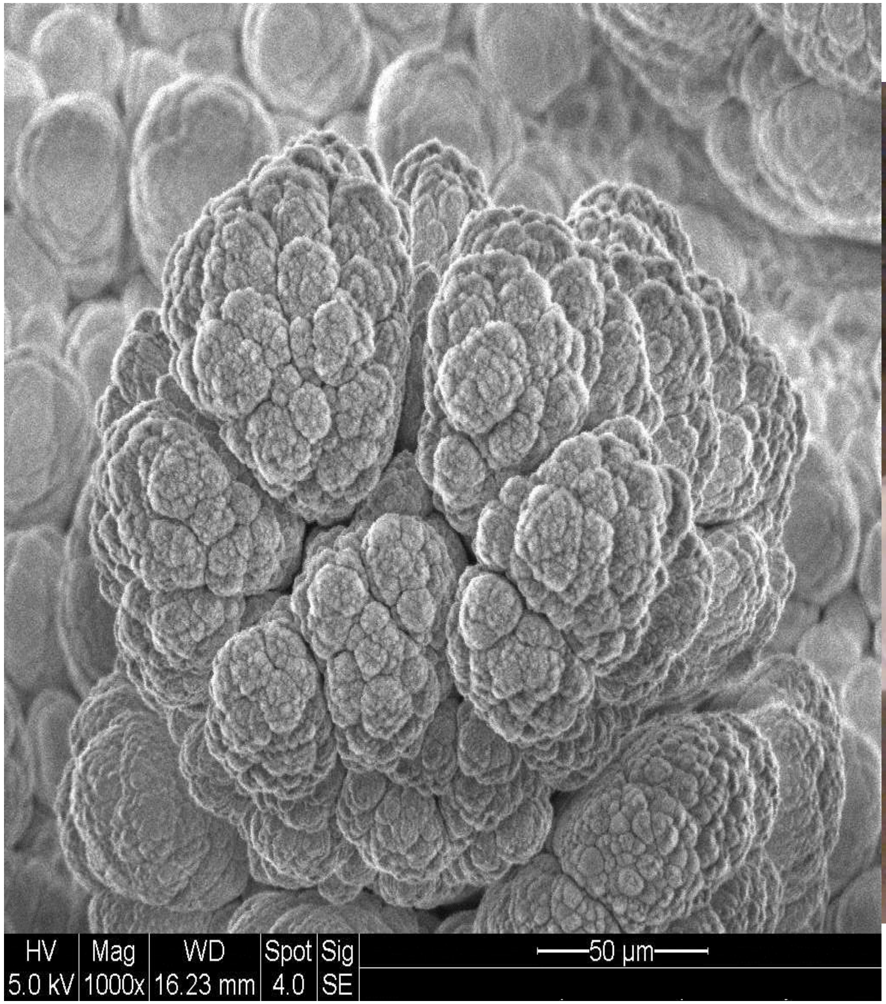

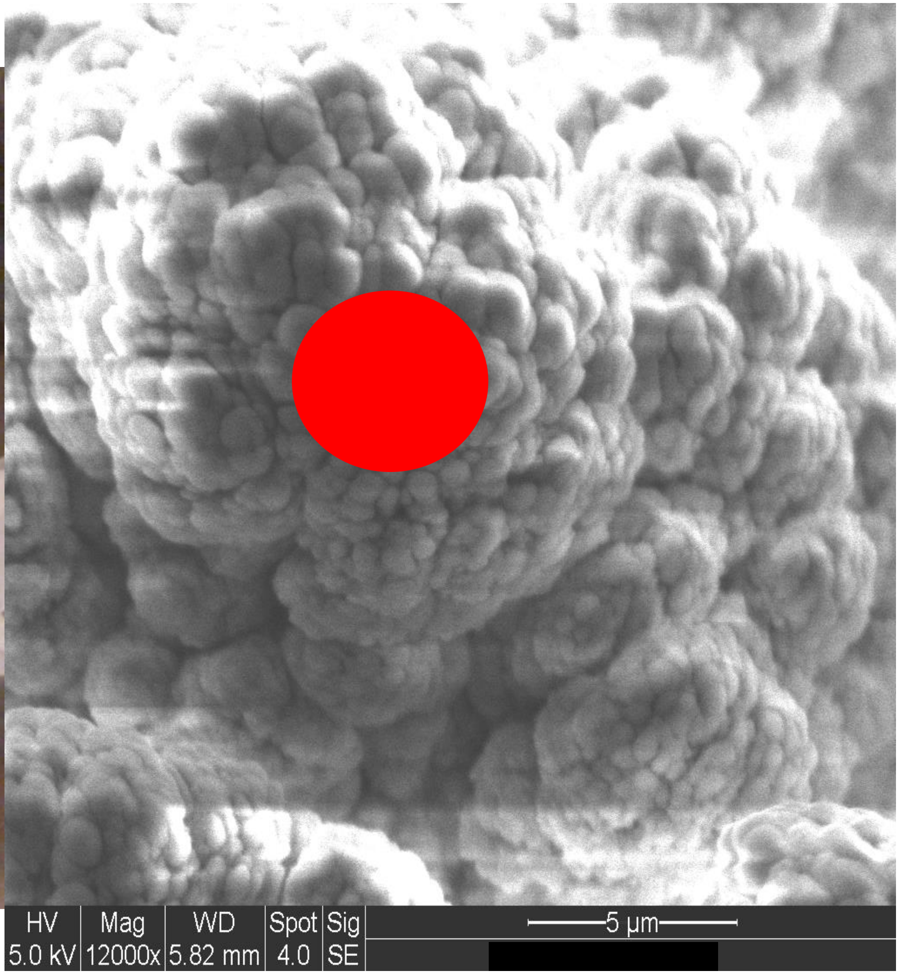

Pre-plasma density spatial profile

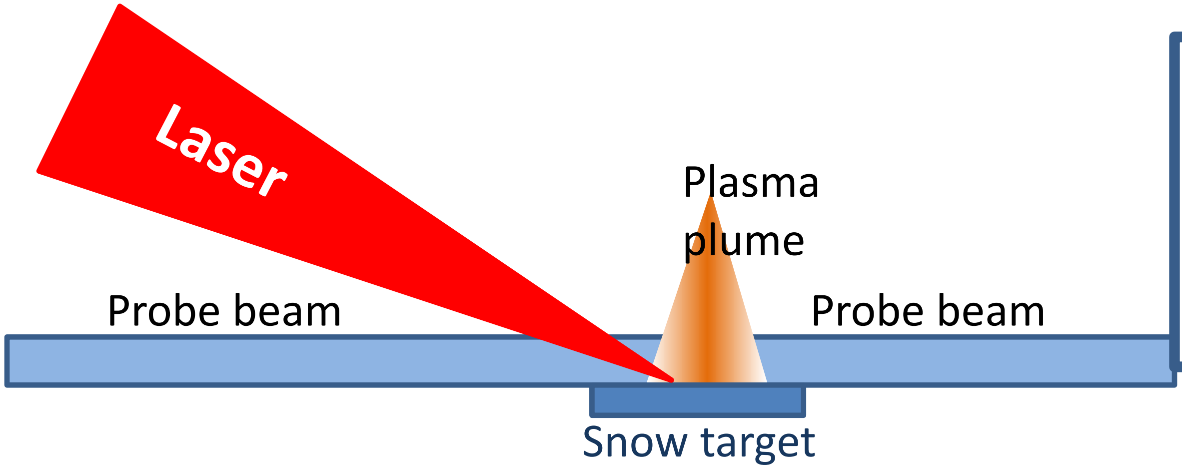

Loyd mirror interferometry and schlieren shadowgraphy

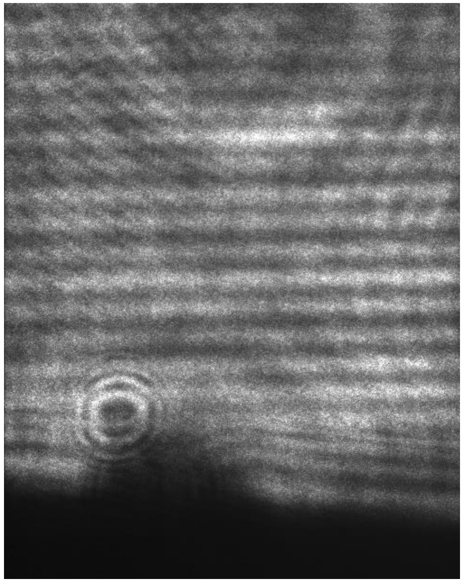

Interferometry Measurements:

Electron density up to $N_e \sim 10^{20}\ cm^{-3}$

Spatial resolution up to 1-3 microns

Output of 1D model - accelerated protons energy

- Field enhancement: $a_{0eff} \sim 3a_0$
- Hot electrons: $$k_B T_h = m_e c^2 \left[\sqrt{1 + \frac{I\lambda^2}{1.37 \cdot 10^{18}}} - 1 \right]$$
- Short length scale: $L \sim 0.05\lambda$
- Accelerating field: $$E_{acc} \approx \frac{kT_{hot}}{eL}$$
- Ion energy: accelerated along one wavelength

$$E_{proton} \cong E_{acc} \times \lambda = 20kT_{hot} = 6MeV$$

At $k_B T_h \sim 300$ keV

Ion acceleration mechanism	Acronym	Ion Accel. process
Target-Normal Sheath Acceleration S. Hatchett *et al.*, Phys. Plas. **7**, 2076 (2000)	TNSA	Charge separation GeV protons? X
Break out afterburner L. Yin *et al.*, Laser Part. Beams **24**, 291 (2006) ; Phys. Plasmas **14**, 056706 (2007)	BOA	Kinetic Process (Buneman): relative *e-i* drift GeV protons? ✓ Linear Polar.
Radiation Pressure Acceleration, Aka Plasma Piston E.g., A.P.L. Robinson, *et al.*, New J. Phys. **10**, 013021 (2008)	RPA	Charge separation GeV protons? ✓ Circular Polar.
Field Enhancement by Microwires Zigler et al PRL 2013	**FEM**	**Charge separation** **150 MeV protons** **by 200 TW**

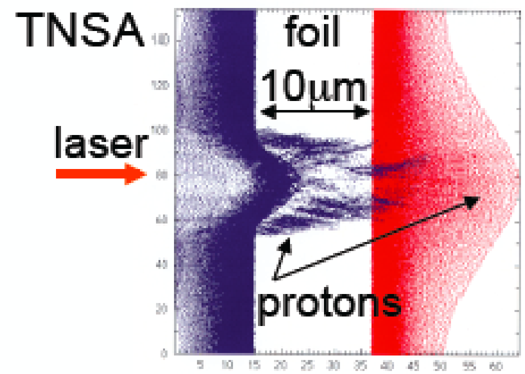

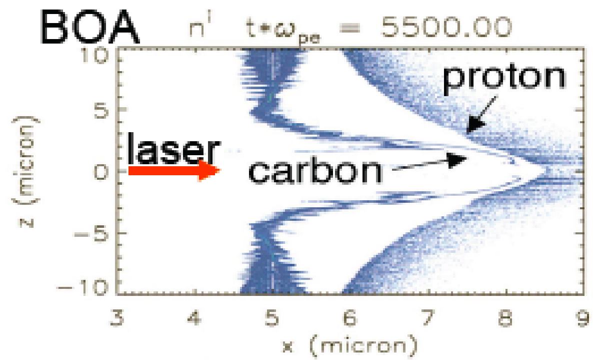

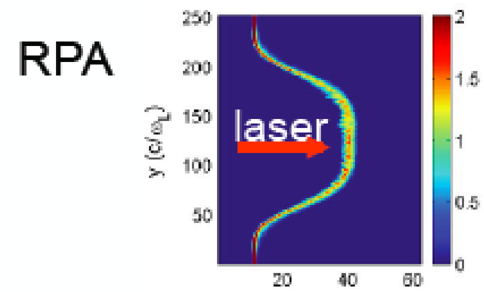

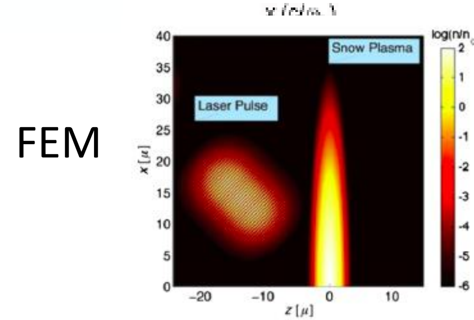

Target- Normal Sheet Acceleration (TNSA)

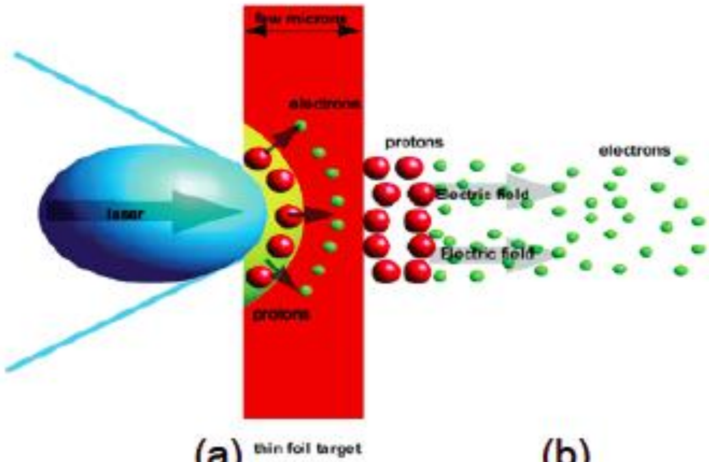

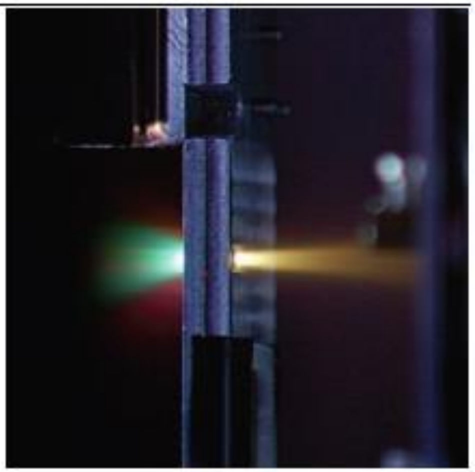

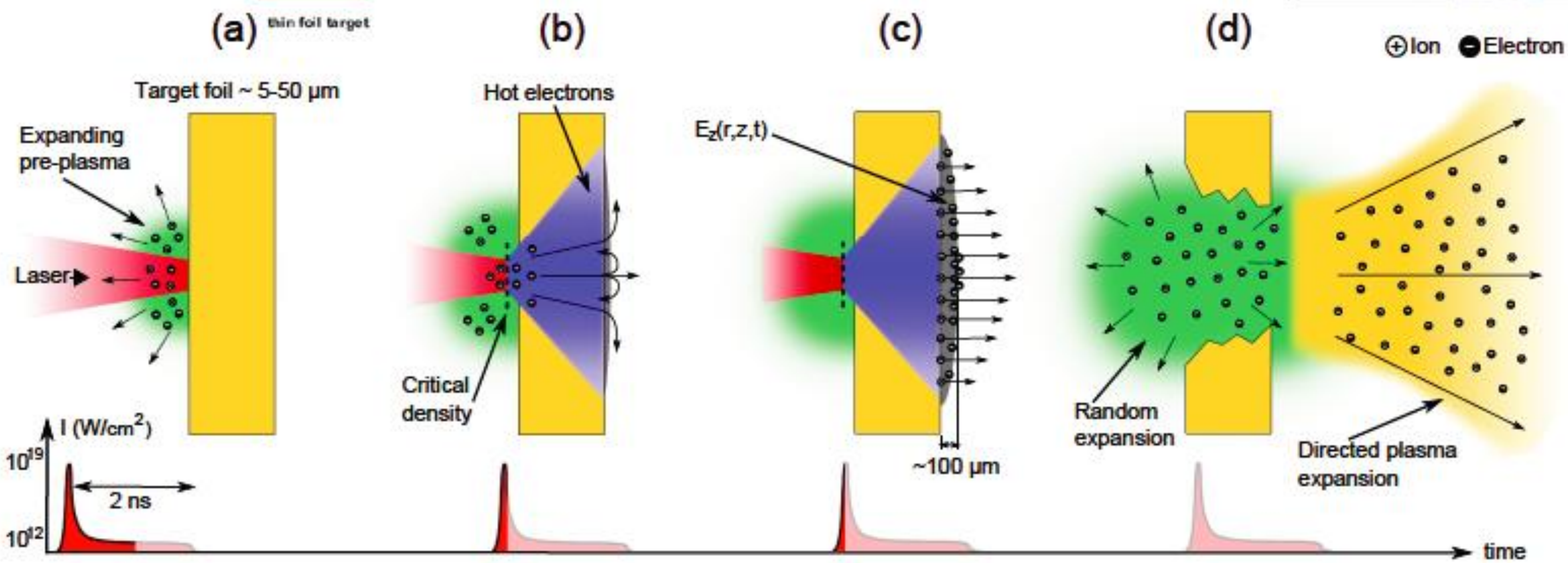

Proton detection setup

- **TOF measurement using a plastic scintillator + PMT provide online energy spectra.**
- **Thomson parabola spectrometer**
- **CR 39 and Cu nuclear activation**

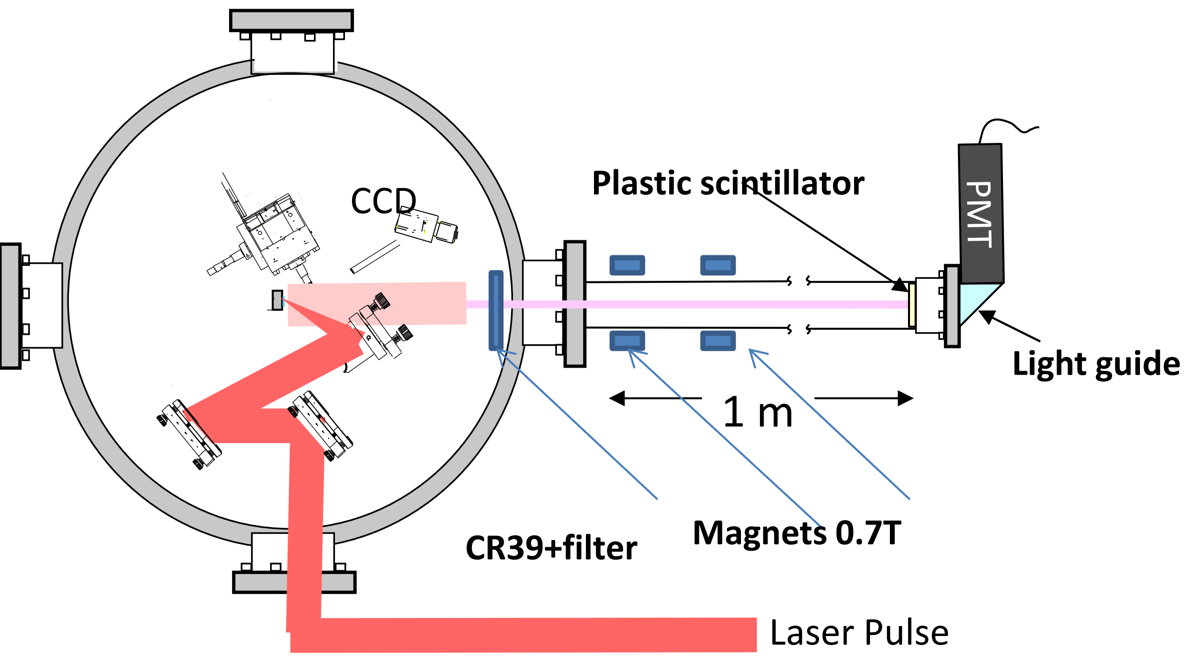

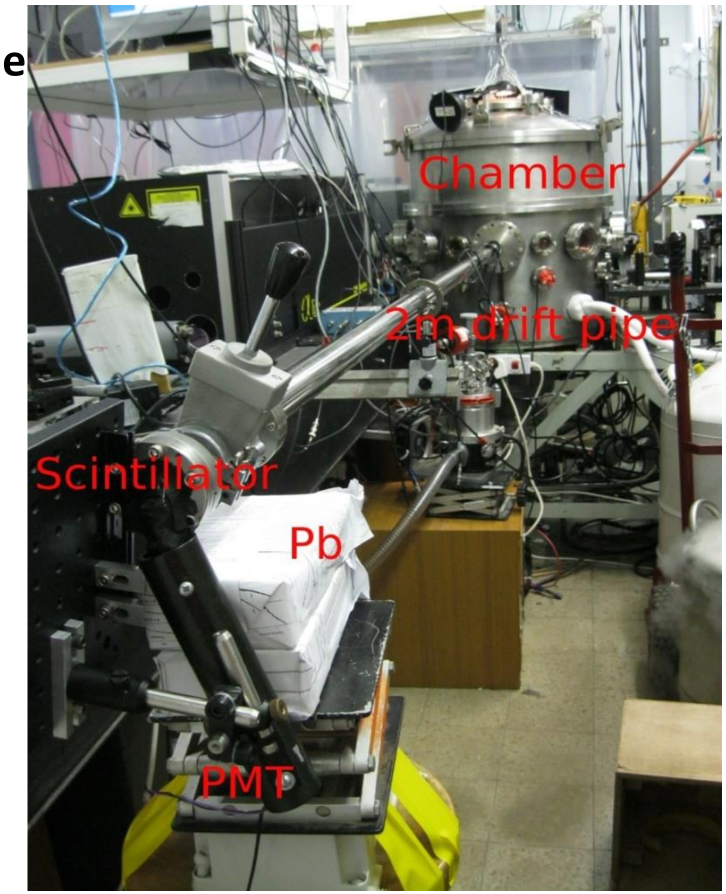

Experiments of proton acceleration with snow targets

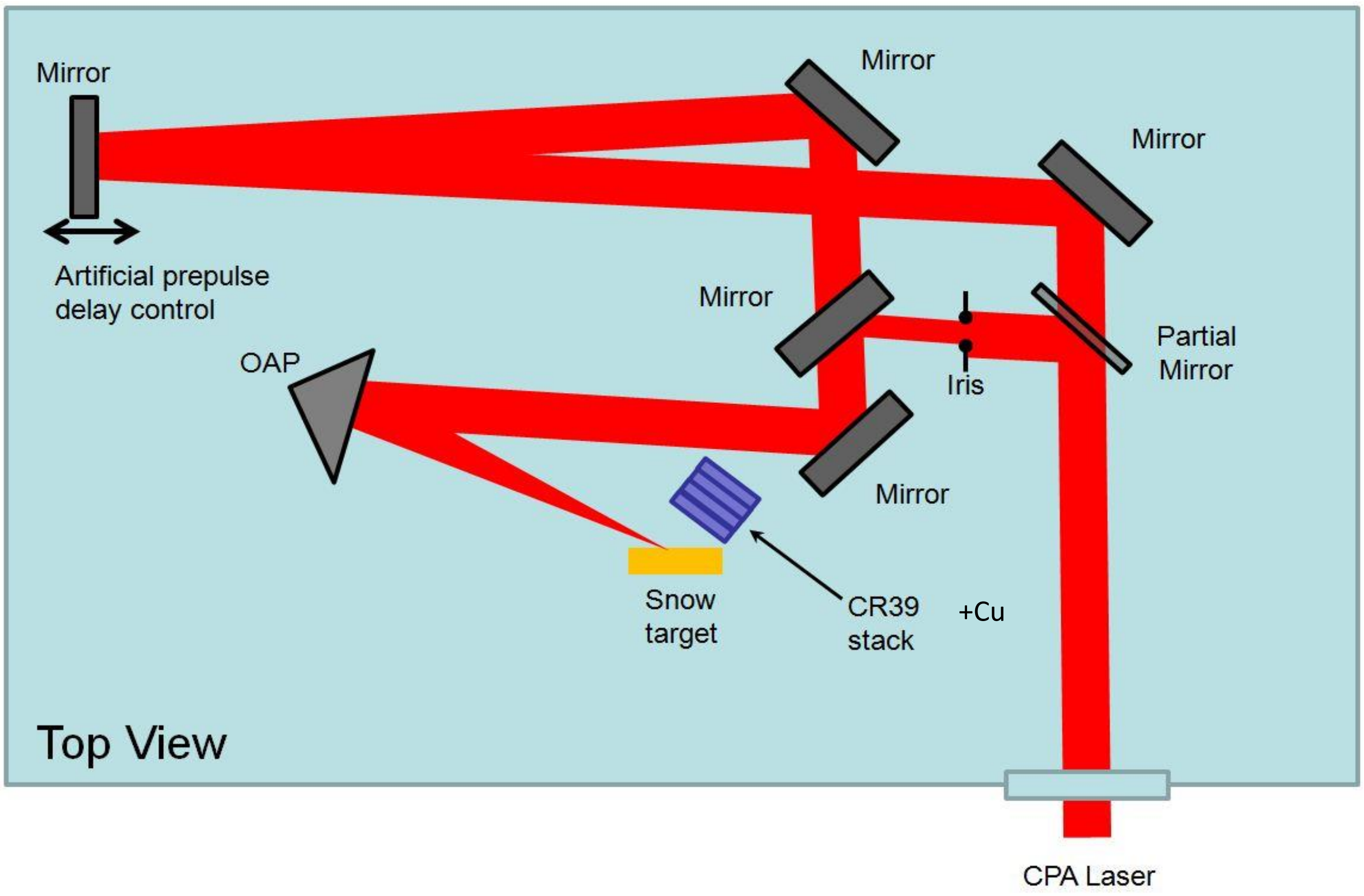

CR39 plates representing typical results of the experiments

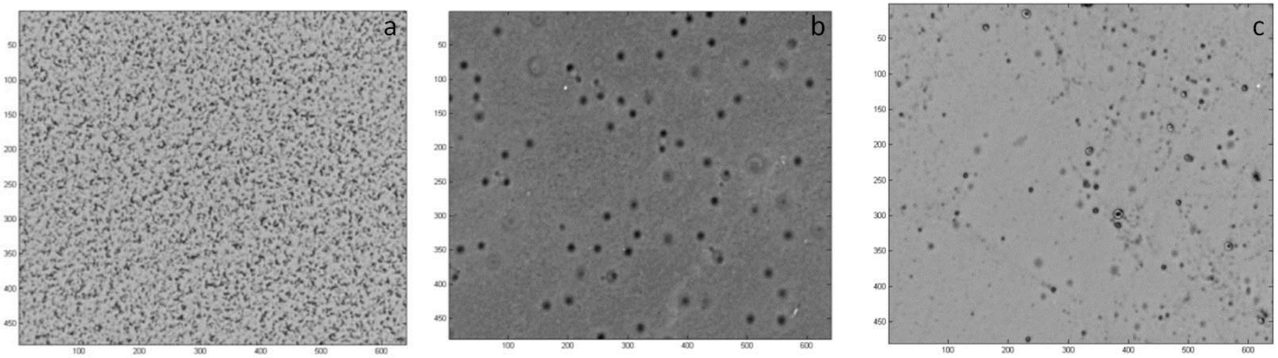

$E_p > 1$ MeV $E_p > 13$ MeV $E_p > 20$ MeV

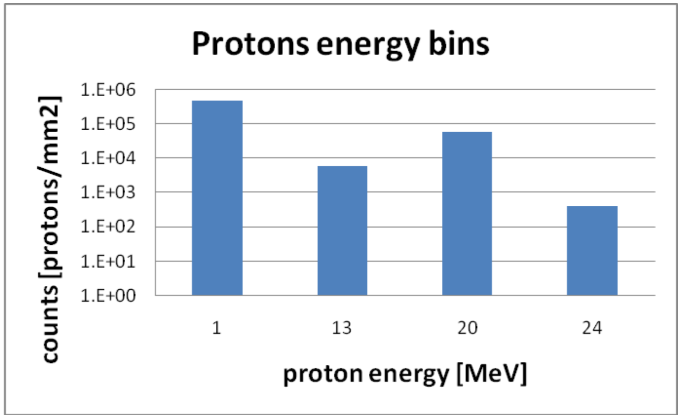

Energy bins – total protons count

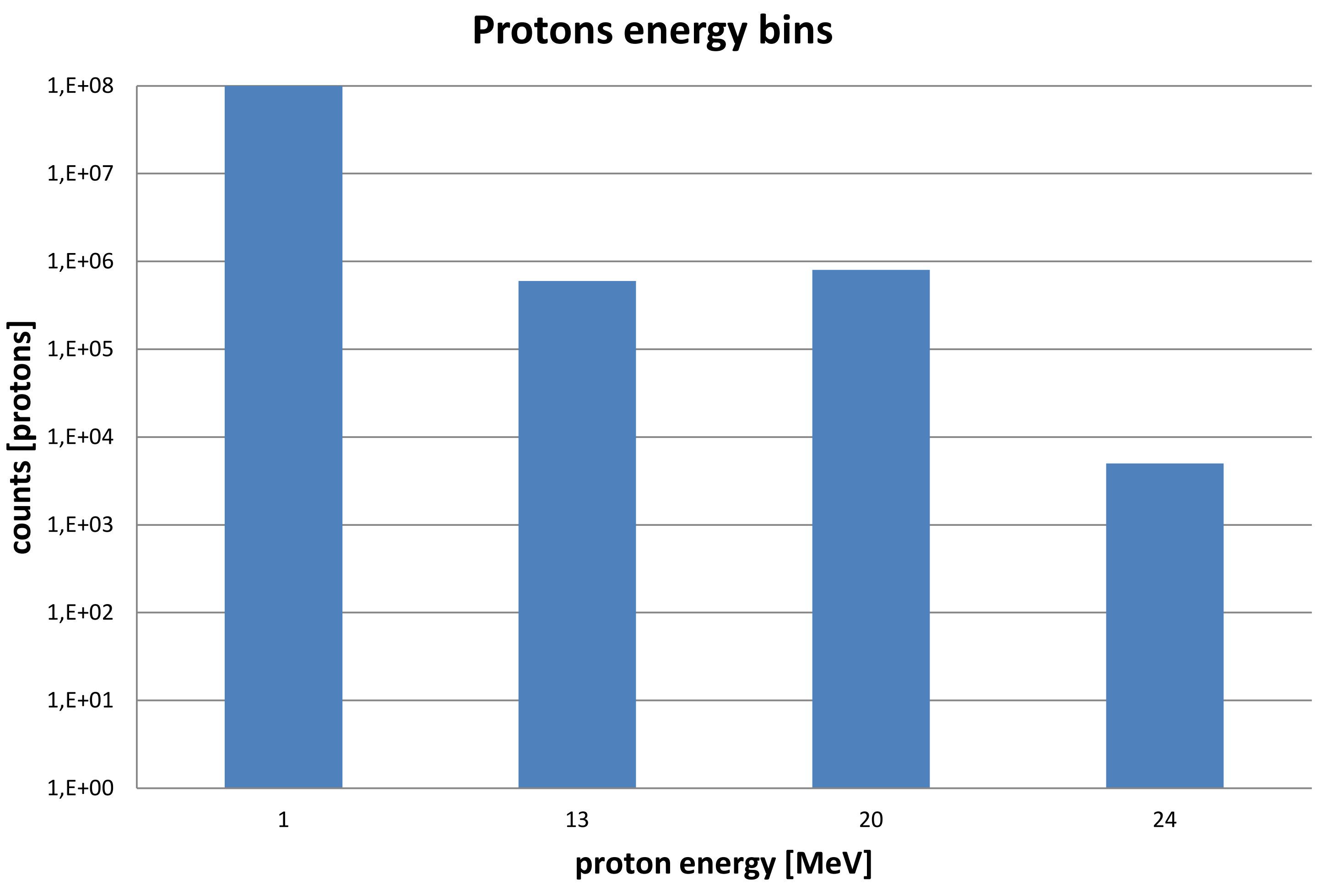

Shot 7354 Texas PW (42TW on Target)

- AR plasma mirrors slides
- Stack (protons arrive from the left):

RCF	Cu	CR39	RCF	Cu	CR39	RCF	Cu	CR39	Cu	CR39	Cu	Cu	CR39	Cu	Cu	CR39	Cu	CR39
	0.5mm	1 mm		0.5mm	1 mm		0.5mm	1 mm	2 mm	1 mm	2 mm	2 mm	1 mm	2 mm	2 mm	1 mm	2 mm	1 mm
	#1	#187		#2	#190		#3	#191	#4	#200	#5	#6	#189	#7	#8	#165	#9	#166

- Geiger counter - Cu#1 signal

Cu Activation (TU)

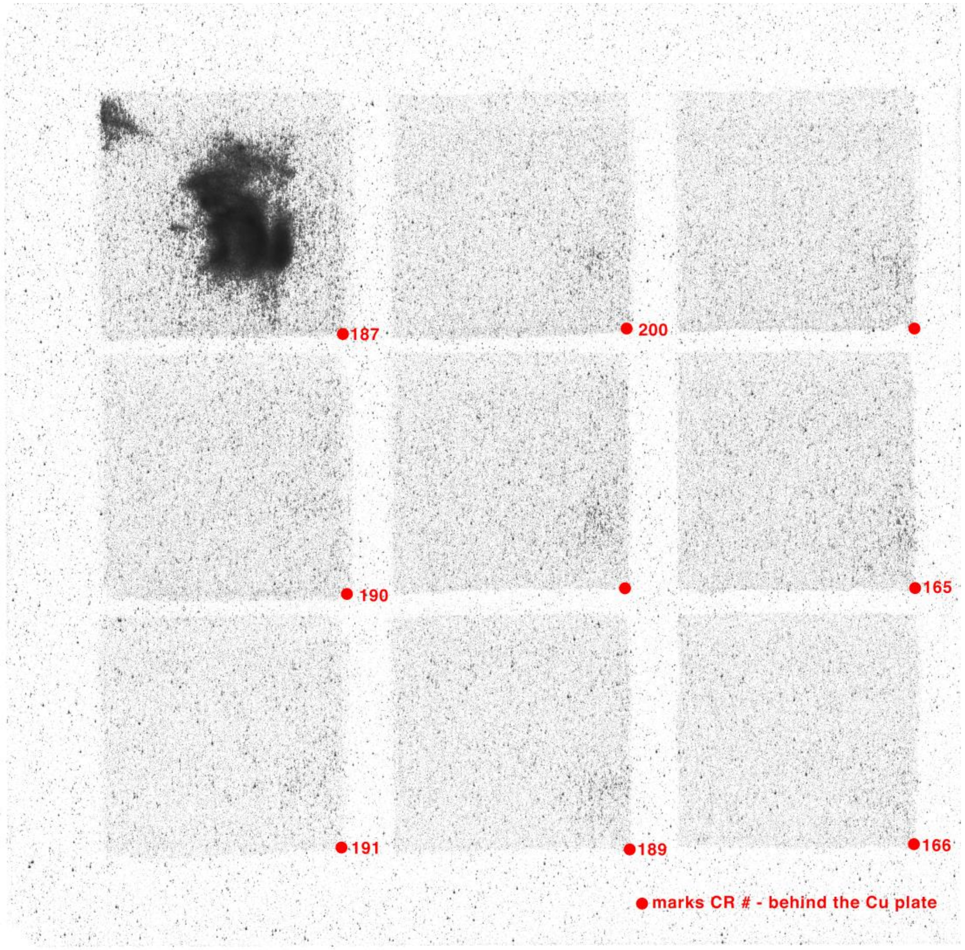

Image plate scan (with grey level adjusted)

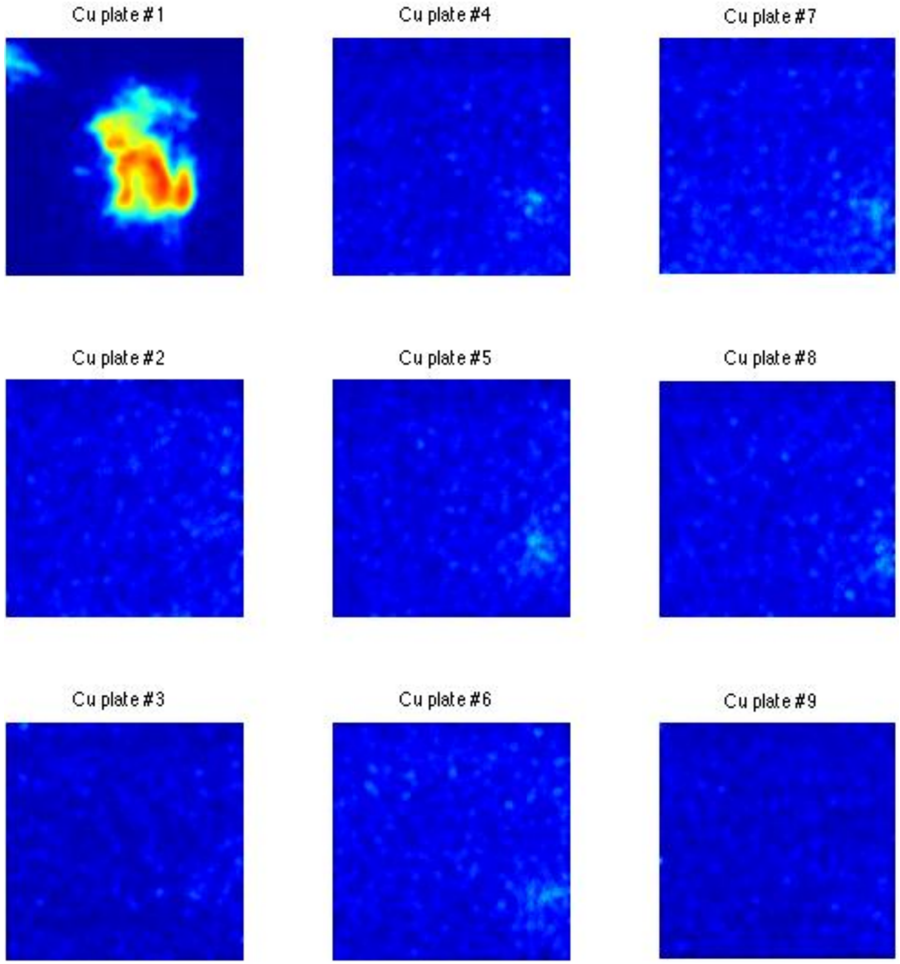

Image plate scan (with spatial 1mm average)

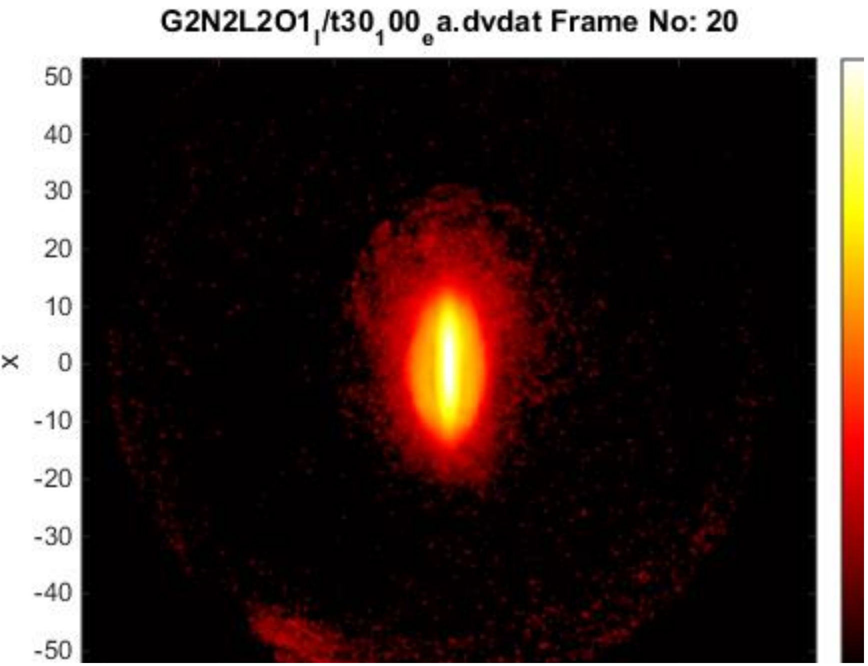

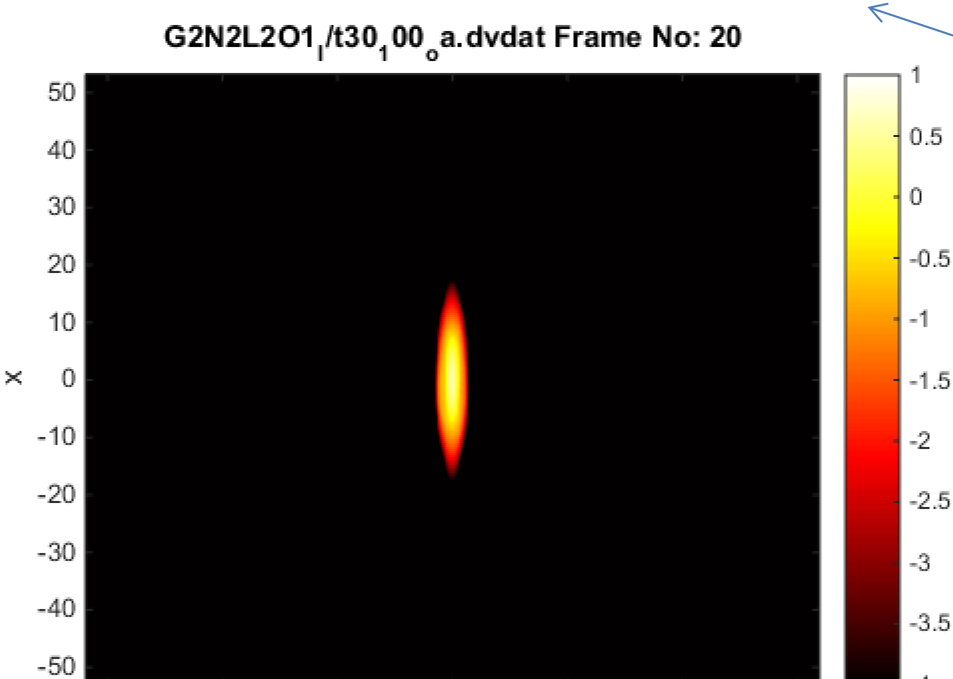

Protons spatial distribution

Electrons spatial distribution

Time: 235 fs after start of interaction, x, z axes in microns

Oxygen ions spatial distribution

$I_L = 2.5 \cdot 10^{19}$ W/cm^2, 90^o irradiance, at 141 fs.

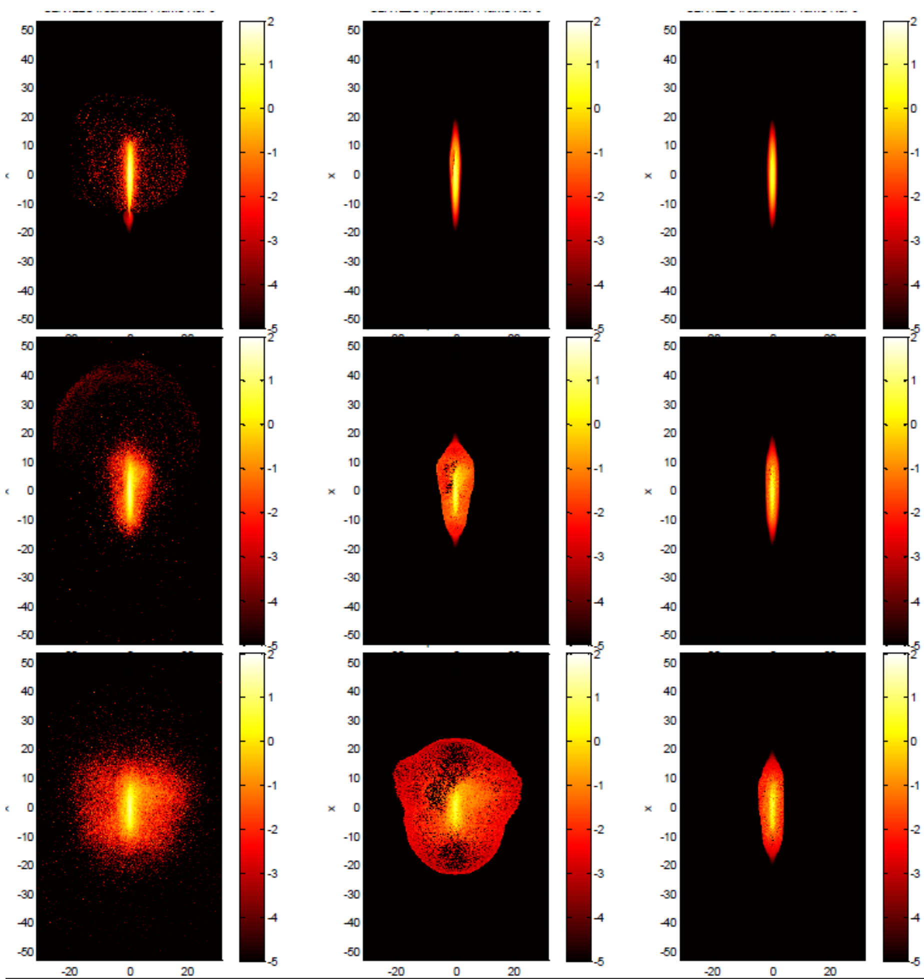

a – 212 fs

b – 424 fs

c – 850 fs

Electrons **Protons** **Oxygen**

Laser-target coupling

Very efficient coupling of laser energy to H_2O layer:

No H_2O deposited on Al_2O_3 (Sapphire)

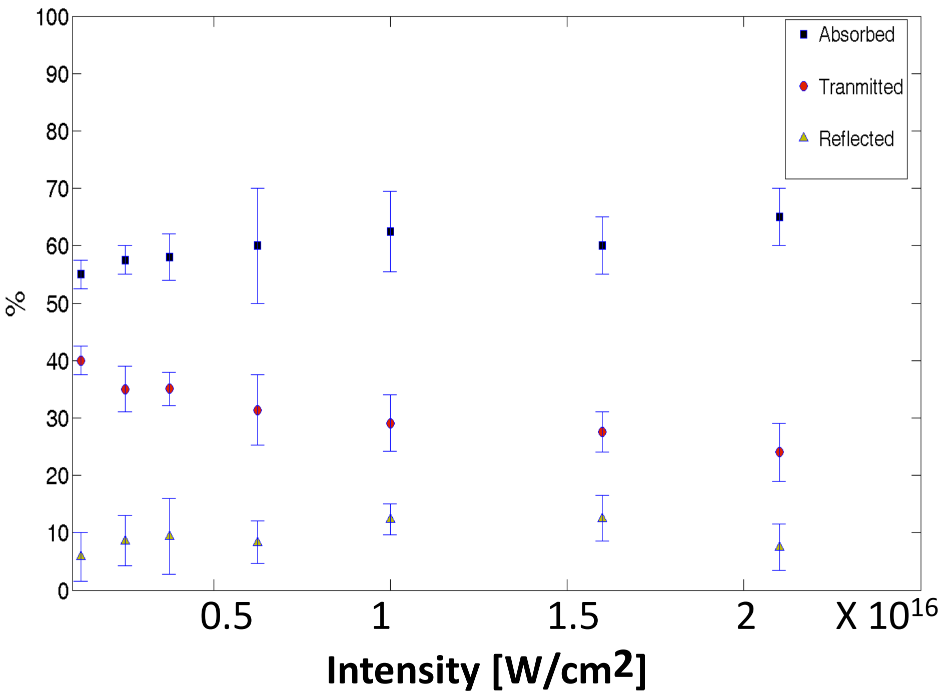

With H_2O deposited on Al_2O_3

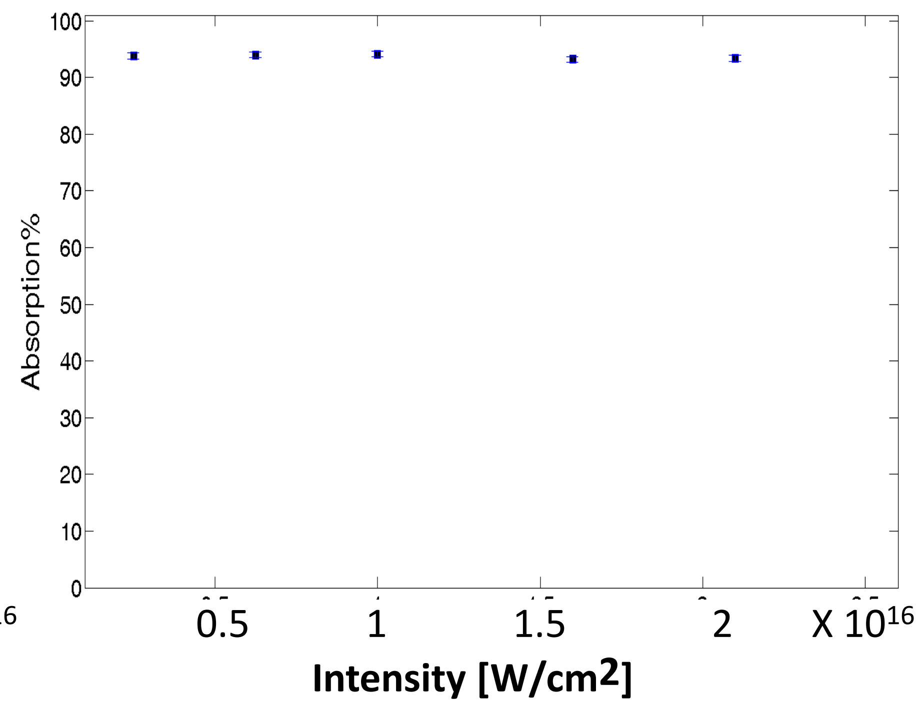

What about the pre pulse?

Energy bins – protons per mm^2 (MBI)

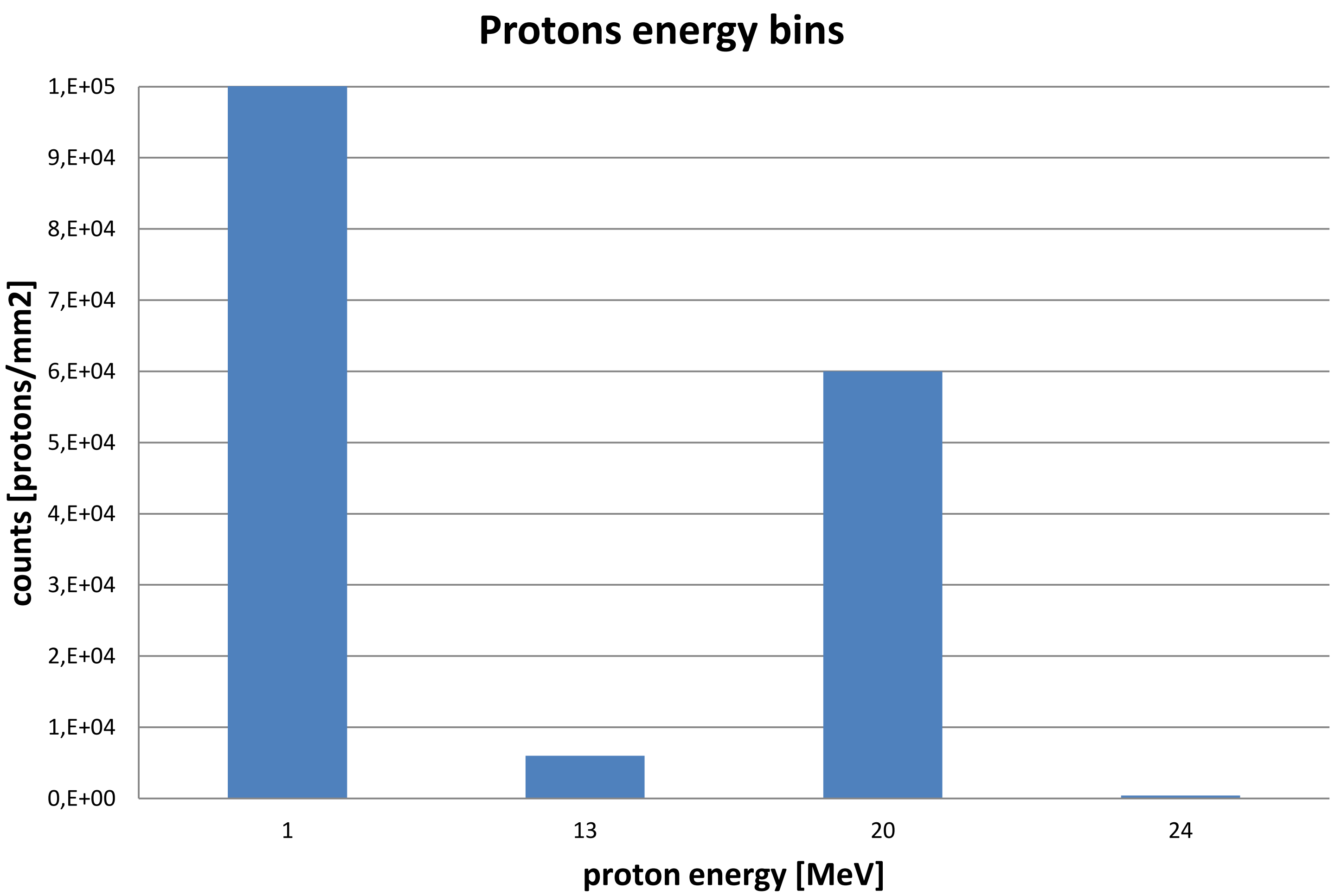

Electric field and protons density distribution along central horizontal line at different times (430 fs – 1138 fs after start of interaction)

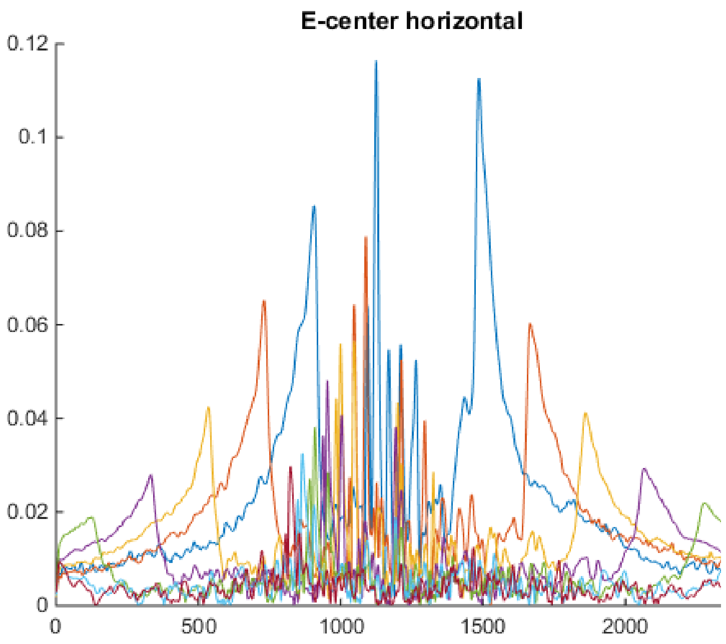

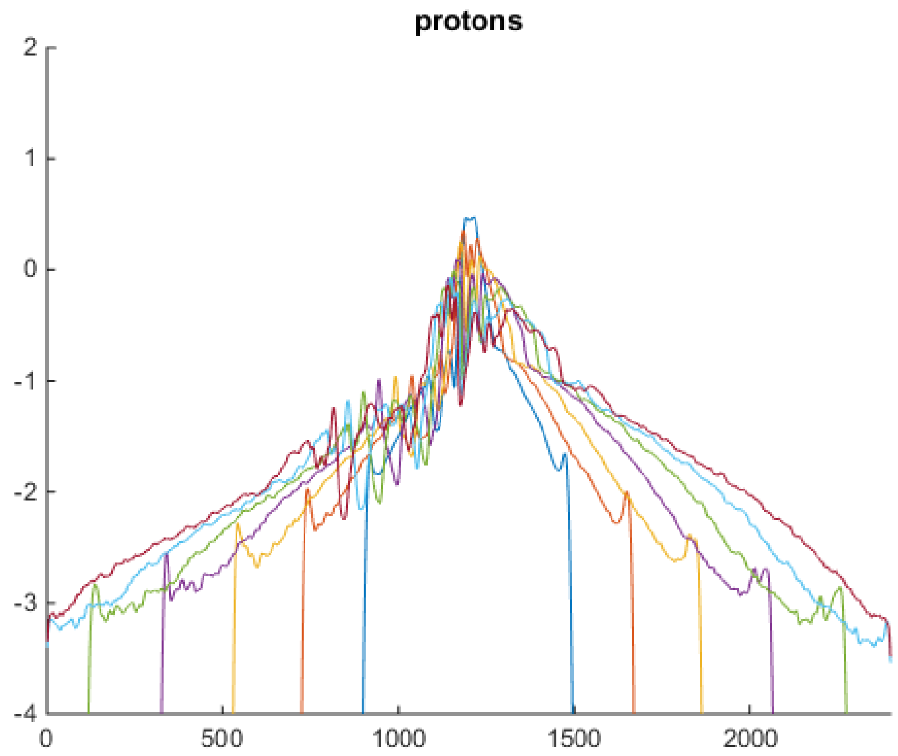

Multi-variables numerical study of the laser – snow whisker interaction

- Different sizes.
- Aspect ratios from 1 to 100.
- Planar and ellipsoid shapes.
- From step-like solid density to under-dense plasma with smooth Gaussian density gradients.
- Laser intensity from $2.5 \cdot 10^{17}$ W/cm^2 to $2.5 \cdot 10^{21}$ W/cm^2 .
- Different angles between the laser propagation and the whisker axis of symmetry.

Pre-plasma density temporal profile

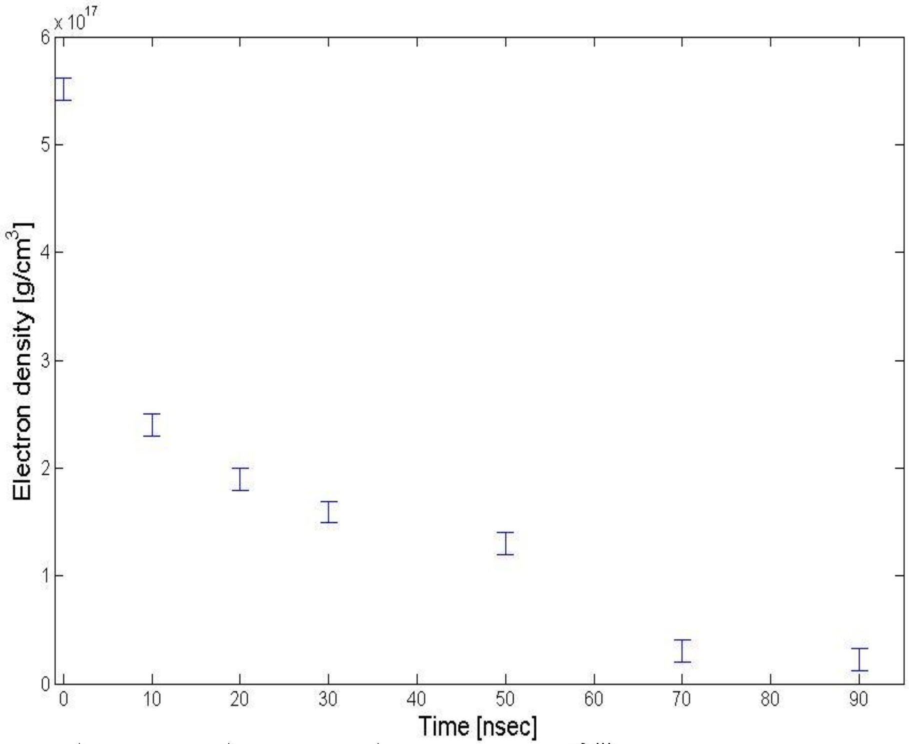

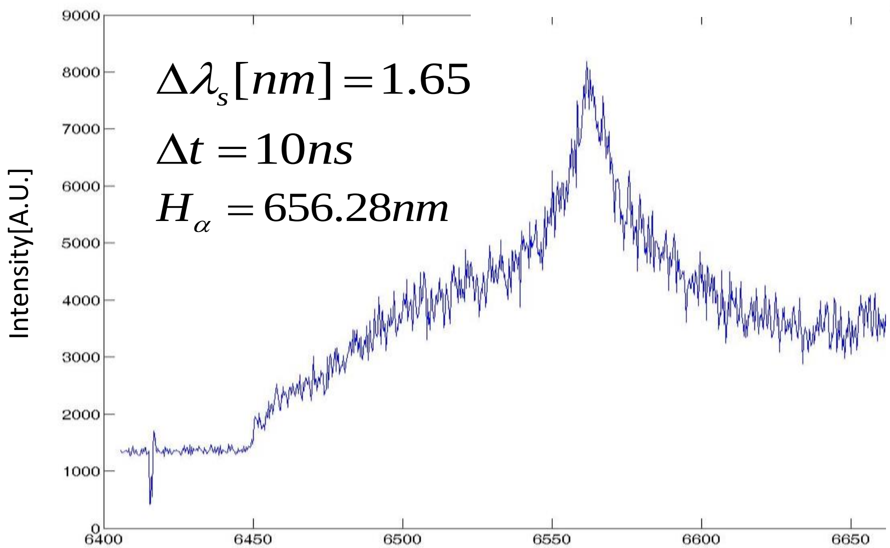

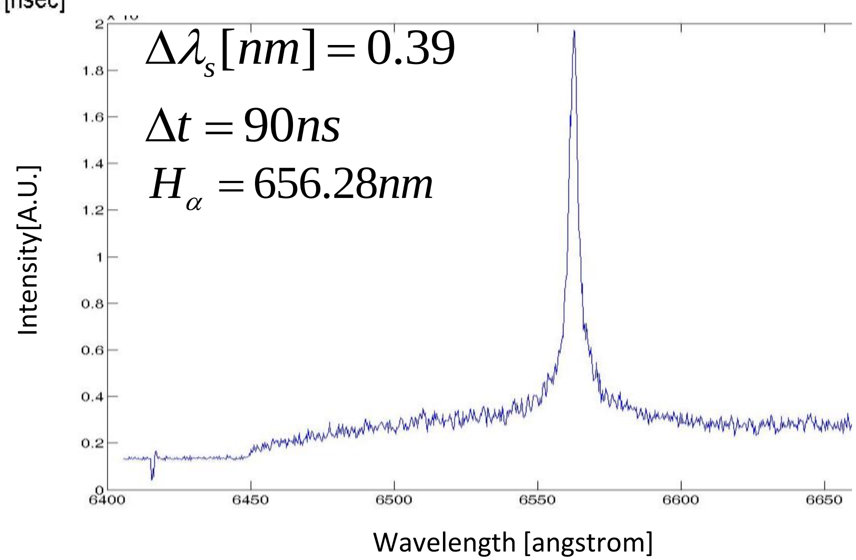

Protons energy spectrum

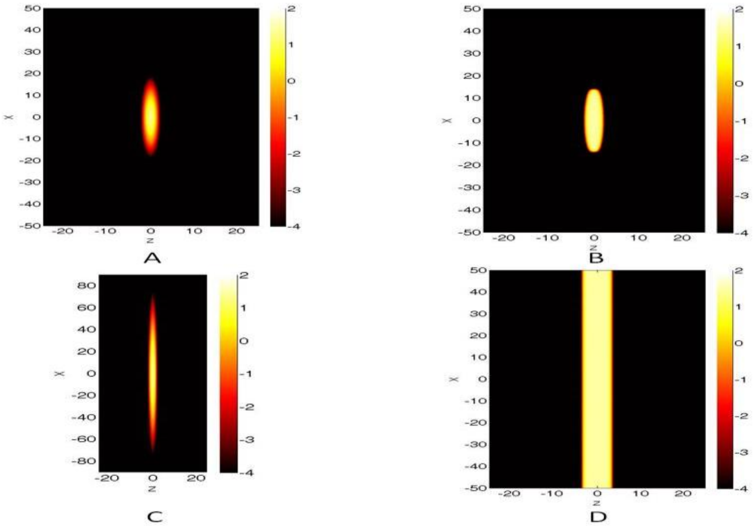

$I_L = 2.5 \cdot 10^{19}$ W/cm^2, propagating at 45º.

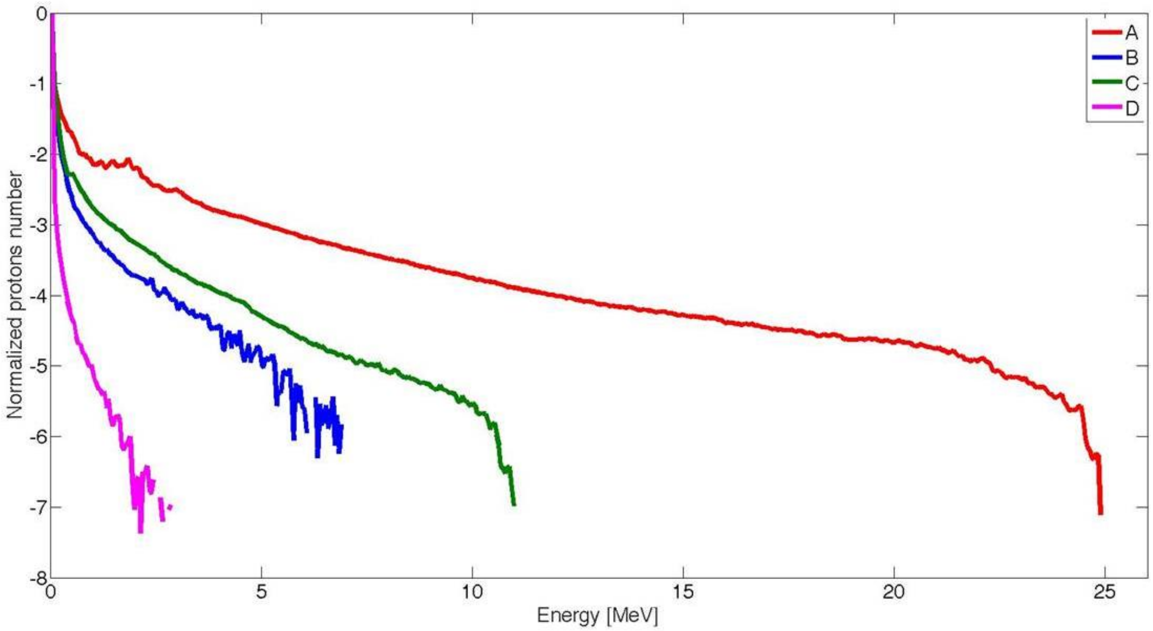

Proton energy vs. laser power (current status)

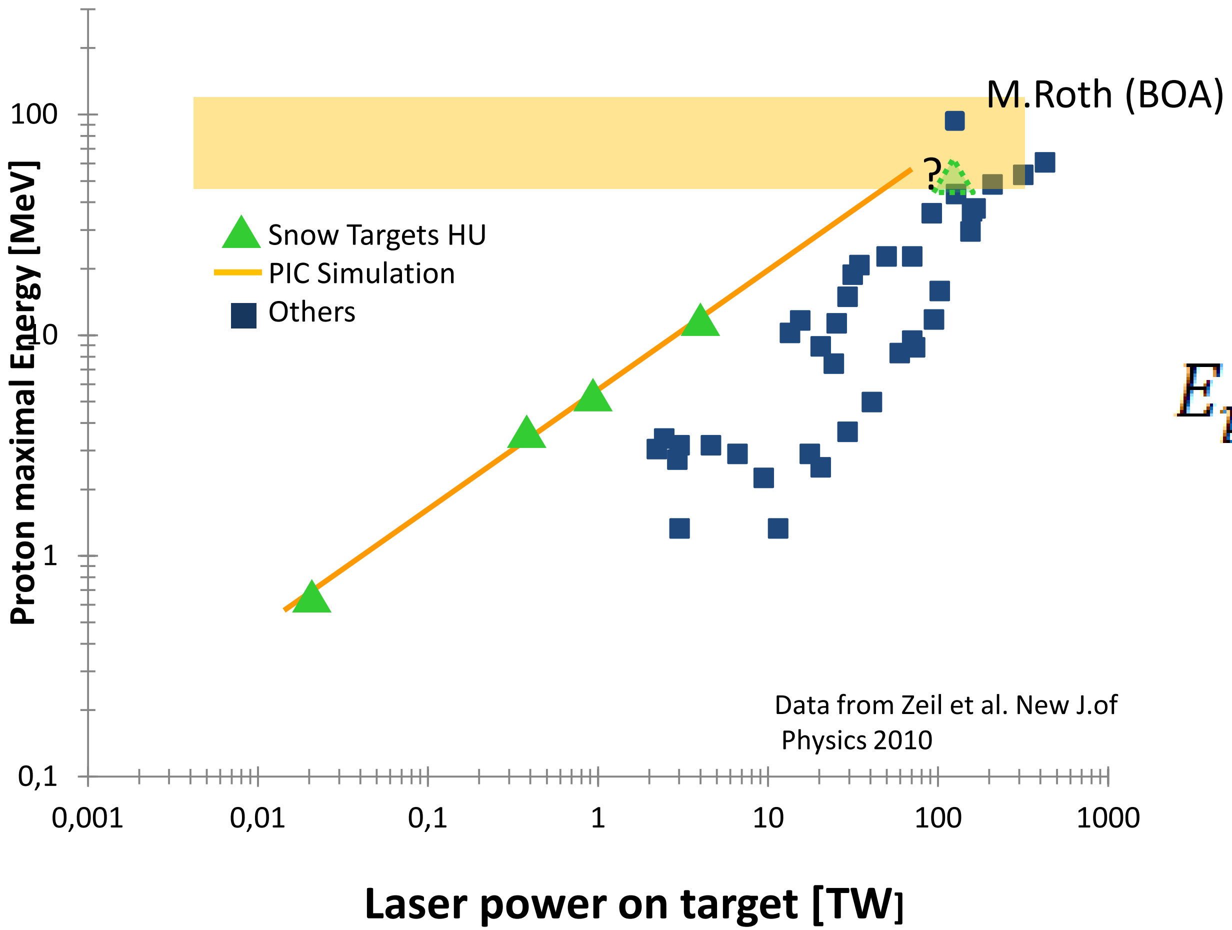

$$E_p \sim P_L^{1/2}$$

Future work

- Experiments with controlled targets.
- Study of the pre-plasma characteristics and impact on proton acceleration.
- Simulation of interaction of the laser with more than one whisker.
- Experiments at laser system with $I>5\ 10^{19} W/cm^2$

  and highly controlled prepulse

Collisionless plasma description

$$
\begin{cases}
\dfrac{\partial f_j}{\partial t} &= -\mathbf{v}\cdot\dfrac{\partial f_j}{\partial \mathbf{x}} - q_j\left(\mathbf{E}+\dfrac{\mathbf{v}}{c}\times\mathbf{B}\right)\cdot\dfrac{\partial f_j}{\partial \mathbf{p}} \\
\nabla\cdot\mathbf{E} &= 4\pi\rho \\
\nabla\times\mathbf{E} &= -\dfrac{1}{c}\dfrac{\partial \mathbf{B}}{\partial t} \\
\nabla\times\mathbf{B} &= \dfrac{4\pi}{c}\mathbf{J}+\dfrac{1}{c}\dfrac{\partial \mathbf{E}}{\partial t} \\
\nabla\cdot\mathbf{B} &= 0
\end{cases}
$$

$$
\begin{aligned}
\rho &= \sum_j q_j \int f_j(\mathbf{x},\mathbf{p},t)\,\mathrm{d}\mathbf{p} \\
\mathbf{J} &= \sum_j \frac{q_j}{m_j}\int \mathbf{p} f_j(\mathbf{x},\mathbf{v},t)\,\mathrm{d}\mathbf{p}
\end{aligned}
$$

Structured snow targets

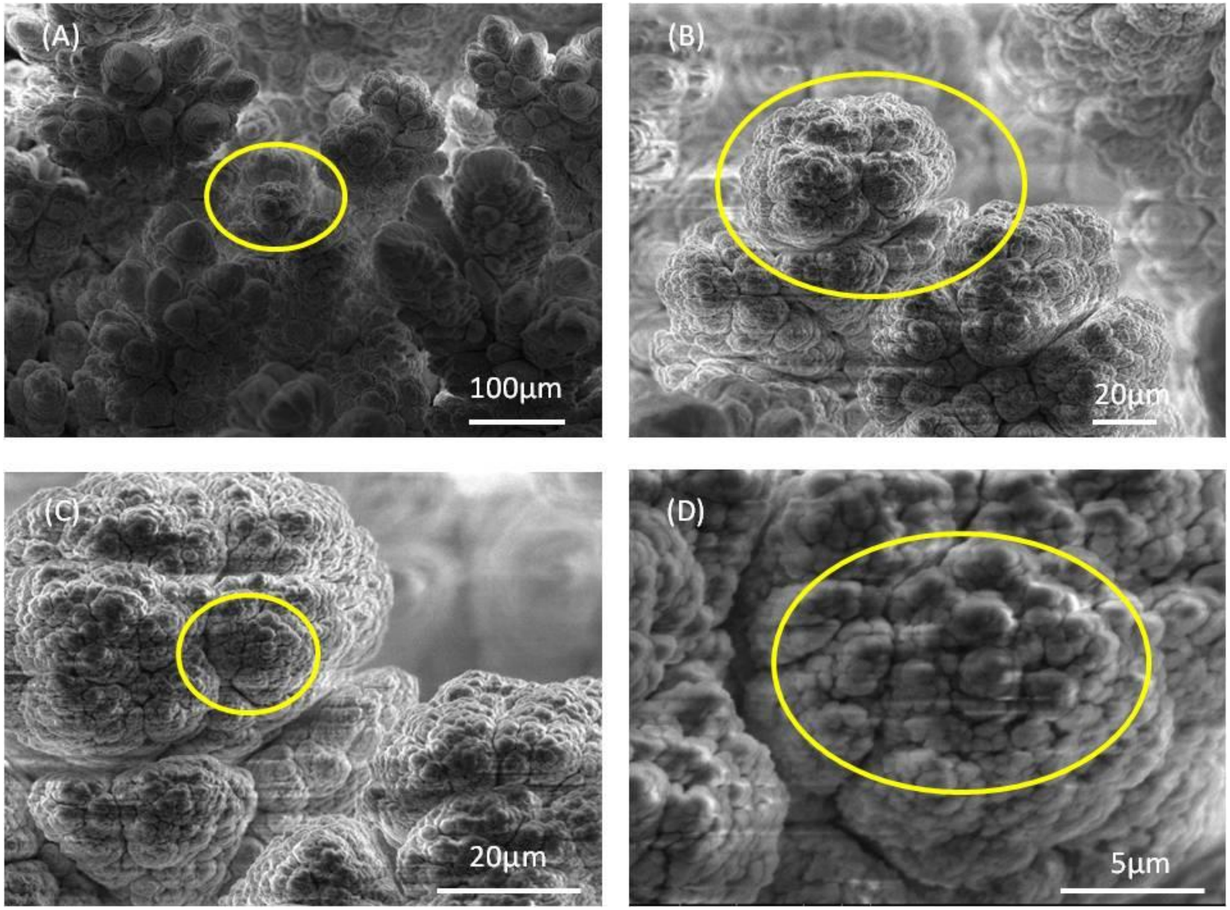

Snow grown in ESEM over a sapphire substrate at -160C at 6 Torr

Schleiffer er all, J. Phys. D, 2015

Relation between Vlasov and macro-particle approach

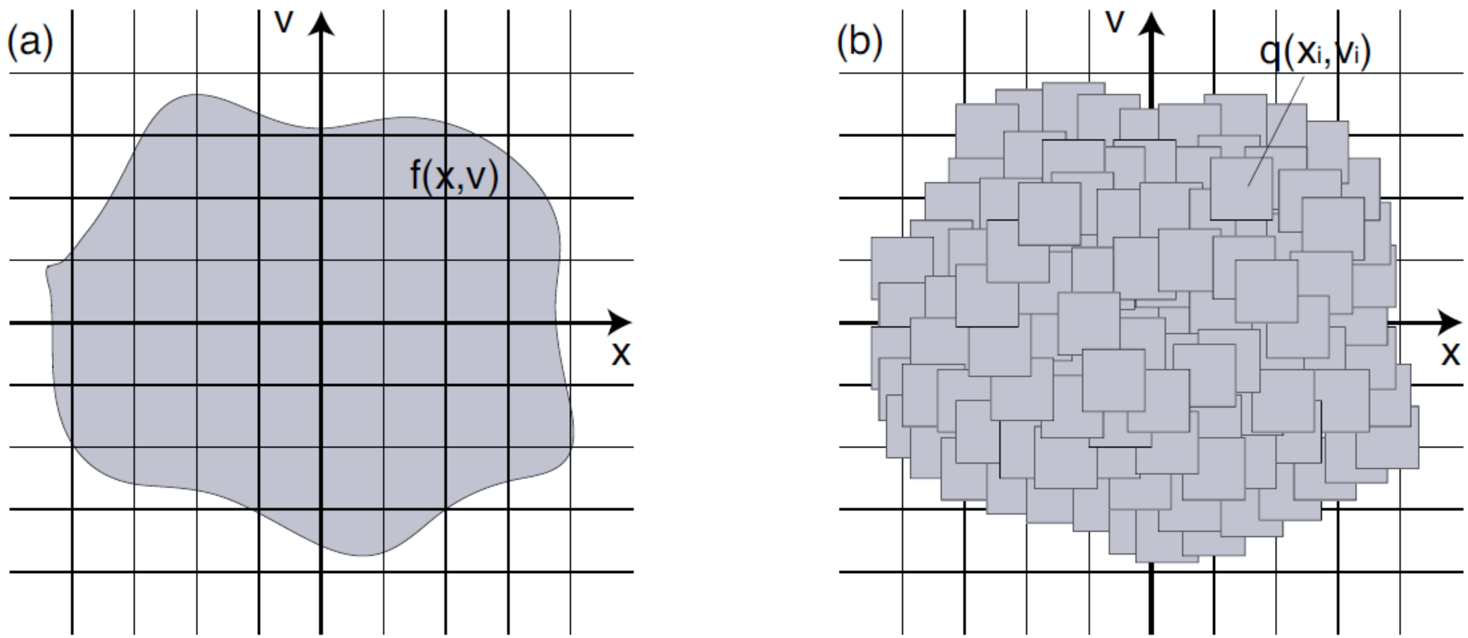

Main loop of a typical PIC code

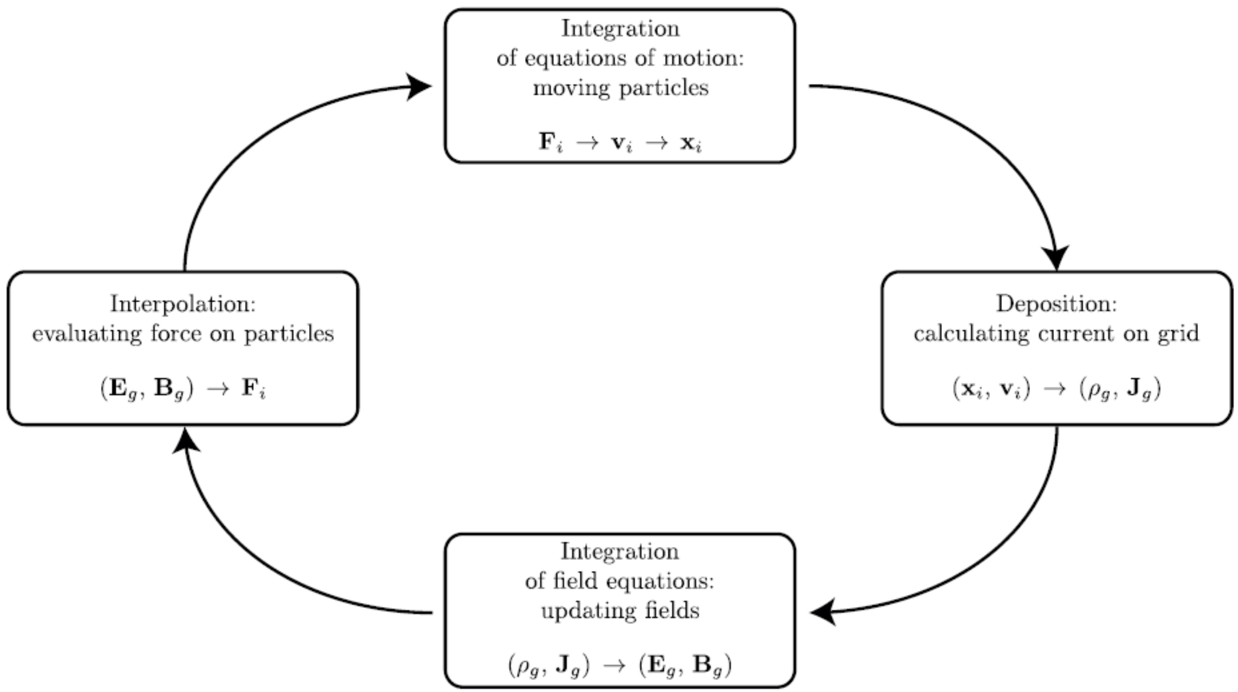

Mechanisms of proton acceleration

- TNSA - target normal sheath acceleration, due to hot electrons.
  - Quasi static models.
  - Plasma expansion.
  - Multi species studies.
- RPA – radiation pressure acceleration, circ. polarization, intensities > 10^{21} W/cm^2 and cleaner pulses.
  - Thick targets: hole boring regime.
  - Thin targets: light sail regime.

- Collisionless shocks.
- Break after burner – transparency regime.
- Field enhancement in structured targets

Motivation

Fundamental research: ion acceleration is a fertile field for theory and simulations.

Current and future applications:

- Proton radiography and imaging
- Production of warm dense matter
- Fast ignition of fusion targets
- Biomedical applications
- Nuclear and particle physics

Recent review articles

- **K. Ledingham et al, NJP 12, 045005 (2010).**
- **H. Daido, Rep. Prog. Phys. 75 , 056401 (2012).**
- **A. Machi, Rev. Mod. Phys. 85, 751, 2013.**

Mechanisms of ion acceleration

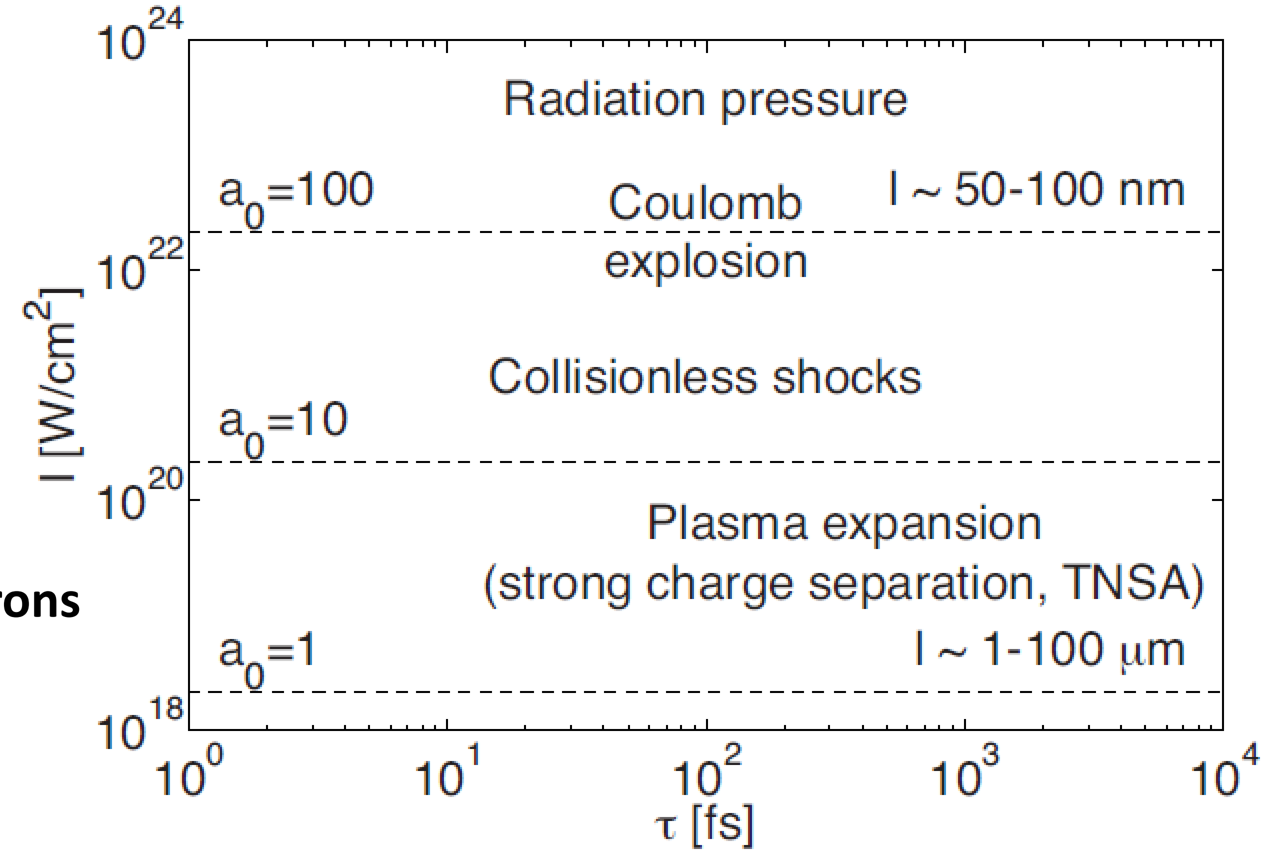

Hot electrons

Boella_Thesis_PhD_UGOV.pdf, 2014

Characterization of the pre plasma
(low density plasma)

Pre pulse schematics

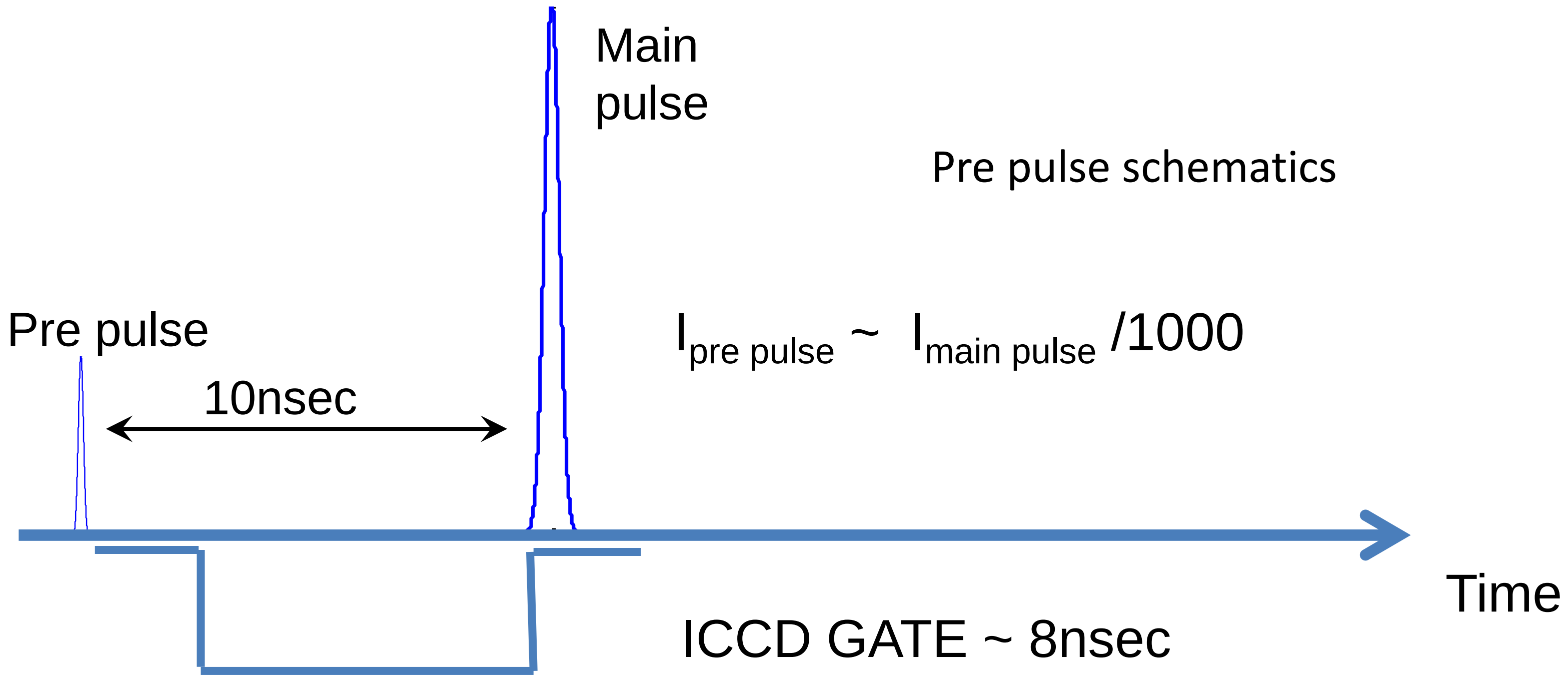

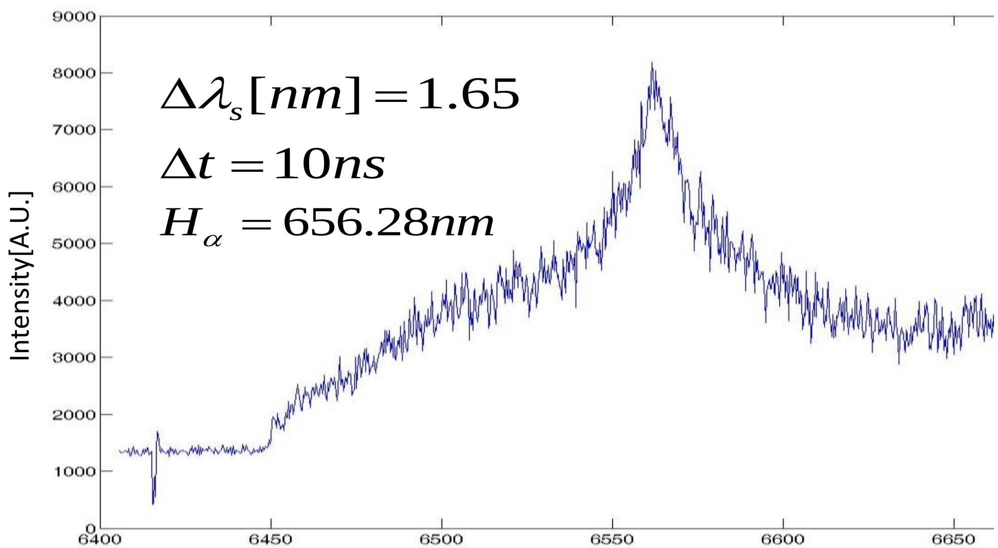

Electron density
$N_e \sim 5*10^{17} cm^{-3}$

CR39 Counting Diagnostics (HU)

90 shots; 2.5cm from target

6MeV filter

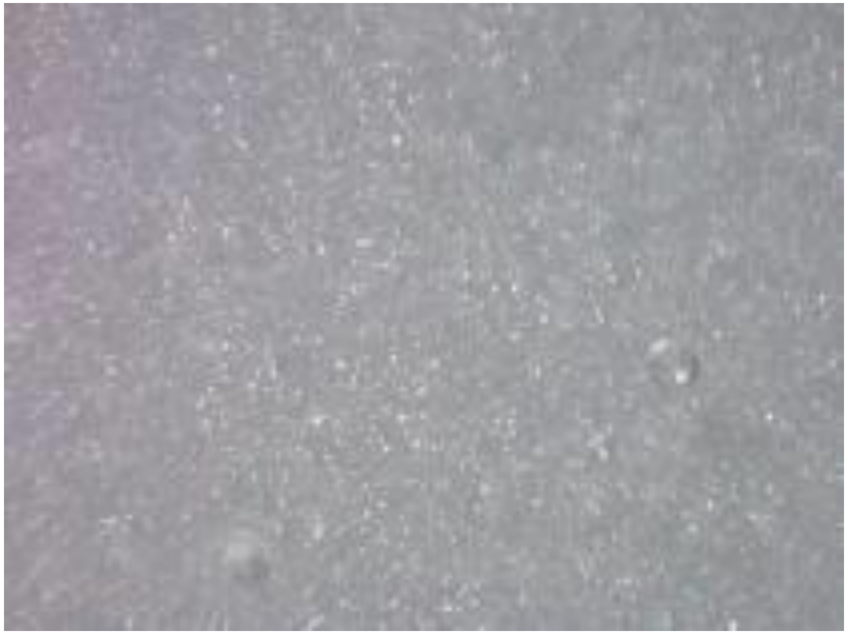

Background

D1 protons >1MeV

- Distribution relatively uniform.
- Counts (based on 30 images) > 2E5 protons/mm^2
- Total counts is 10^8 protons

FOV is 100um

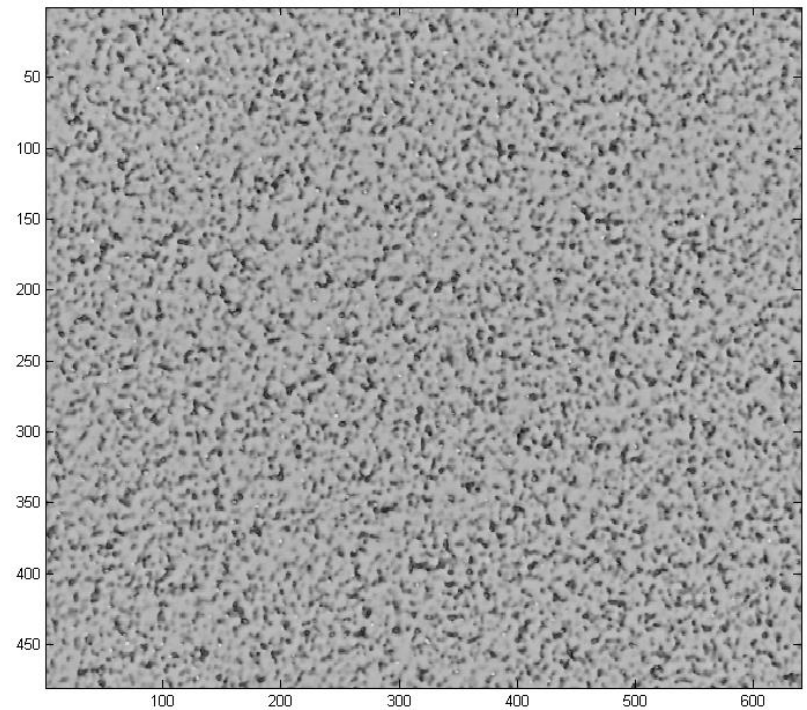

D3 proton > 20 MeV

- Highly non-uniform (bunch)
- Counts (average 30 images) : 10^5 protons/mm^2
- Total count ~ 10^6

FOV is 100um

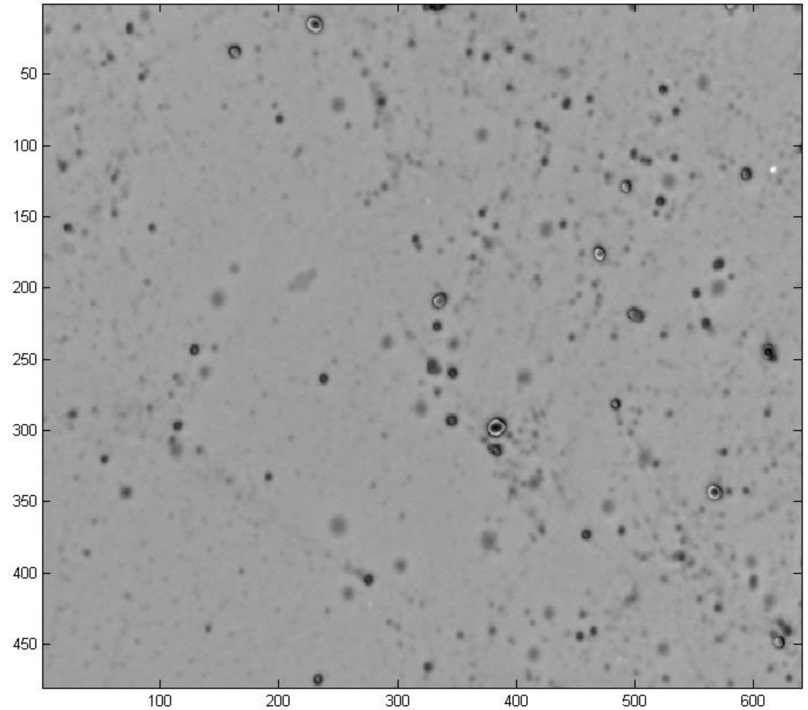

CR39 Counting Diagnostics

Energy Bin* [MeV]	Total proton count	Angular distribution [deg]
1-5	1.00E+08	±35
13-14.5	5.00E+06	±22
20-21	1.00E+06	Bunches (2-5)
80-90**	1.00E+04 ???	Bunch 5

- * Energy bins are not continues due to CR39 detection limits.
- ** Cu activation

1D fluid equations for electrons and protons model

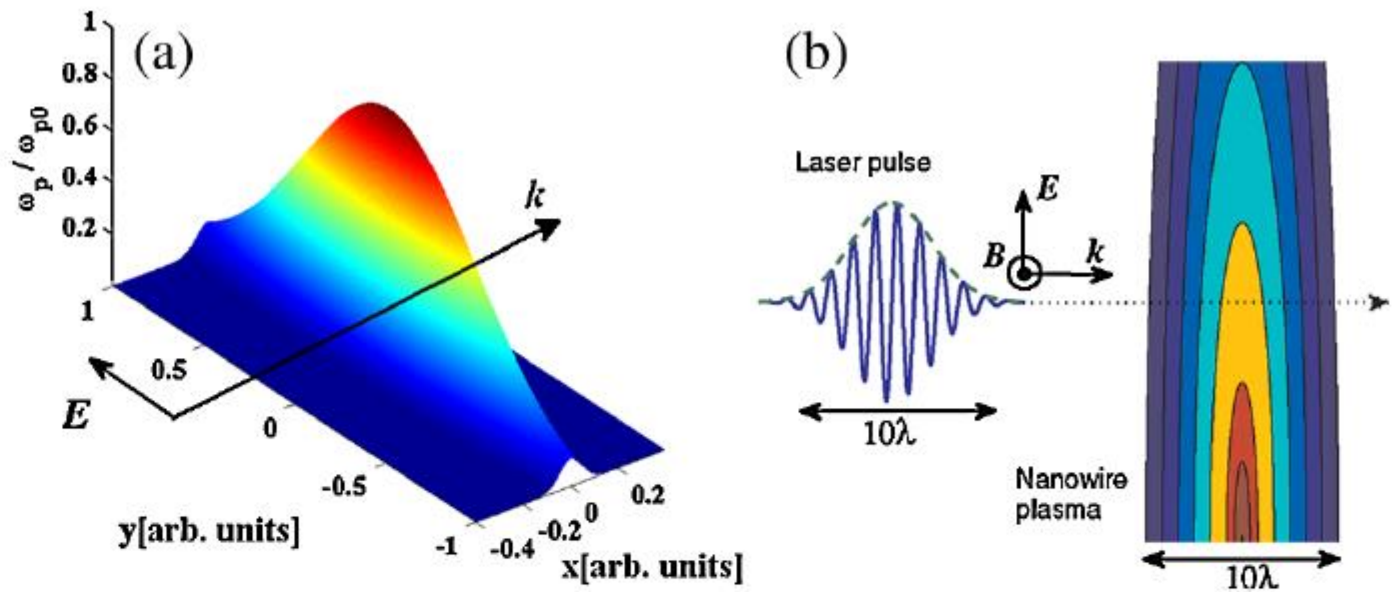

FIG. 3 (color online). (a) The plasma density as a function of planar distance from the original position of the nanowire ($x = 0$, $y = 0$). (b) The laser electric field E propagation through the nanoplasma at a direction k.

TNSA

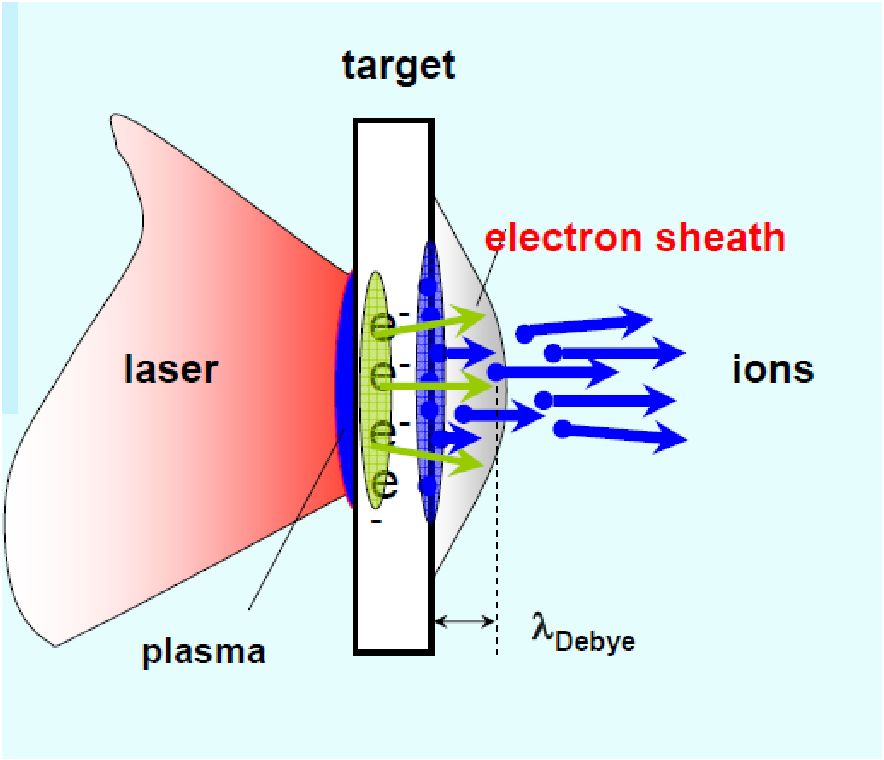

Efficient production of hot electrons, 30%.
Ions are pulled out by the sheath electric field at the rear surface.

$$k_B T_h = m_e c^2 [\sqrt{1 + \frac{I\lambda^2}{1.37 \cdot 10^{18}}} - 1]$$

$$E_{acc} \approx \frac{kT_{hot}}{eL} \qquad L = \lambda_{Debye} = \sqrt{\frac{k_B T_h}{4\pi e^2 n_h}} \qquad n_h = \frac{\eta E_L}{k_B T_h} \frac{1}{Sc\tau_L} = \frac{\eta I_L}{k_B T_h c}$$

1D fluid model... (cont.)

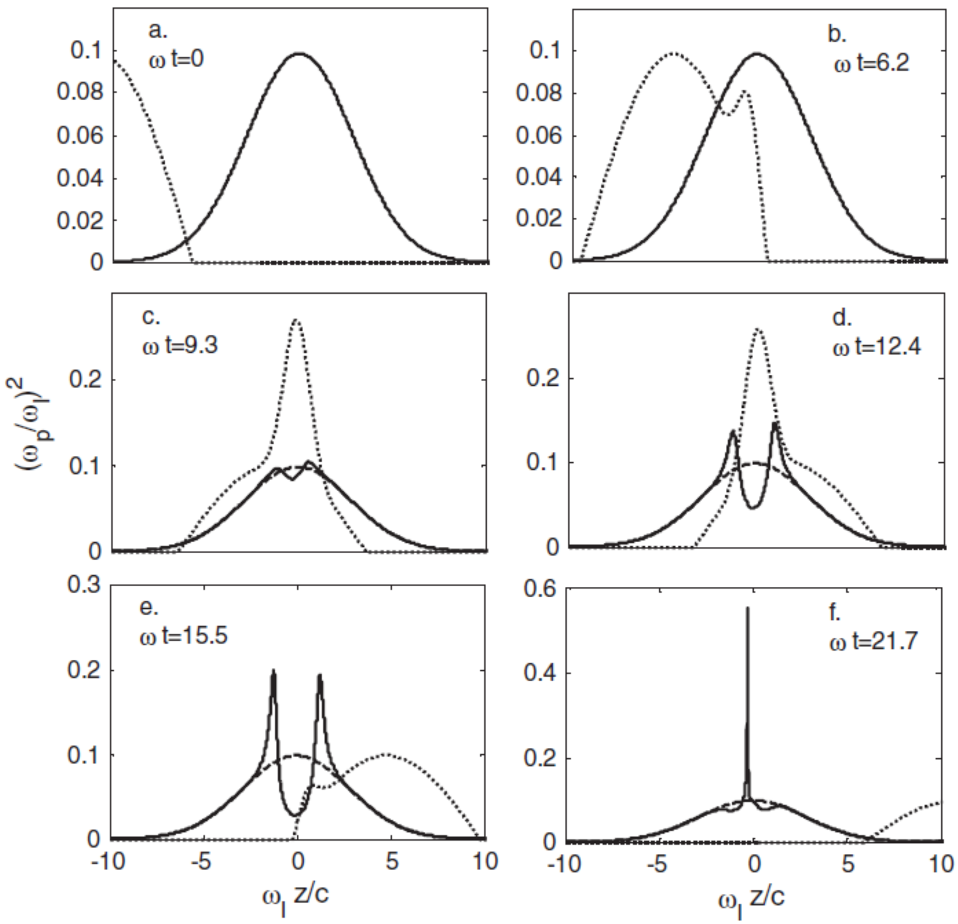

FIG. 5. The density of the electrons (solid line) at six time frames. The laser envelope (dotted line) is enhanced by the NPC. Broken lines show the initial distribution of the electrons.

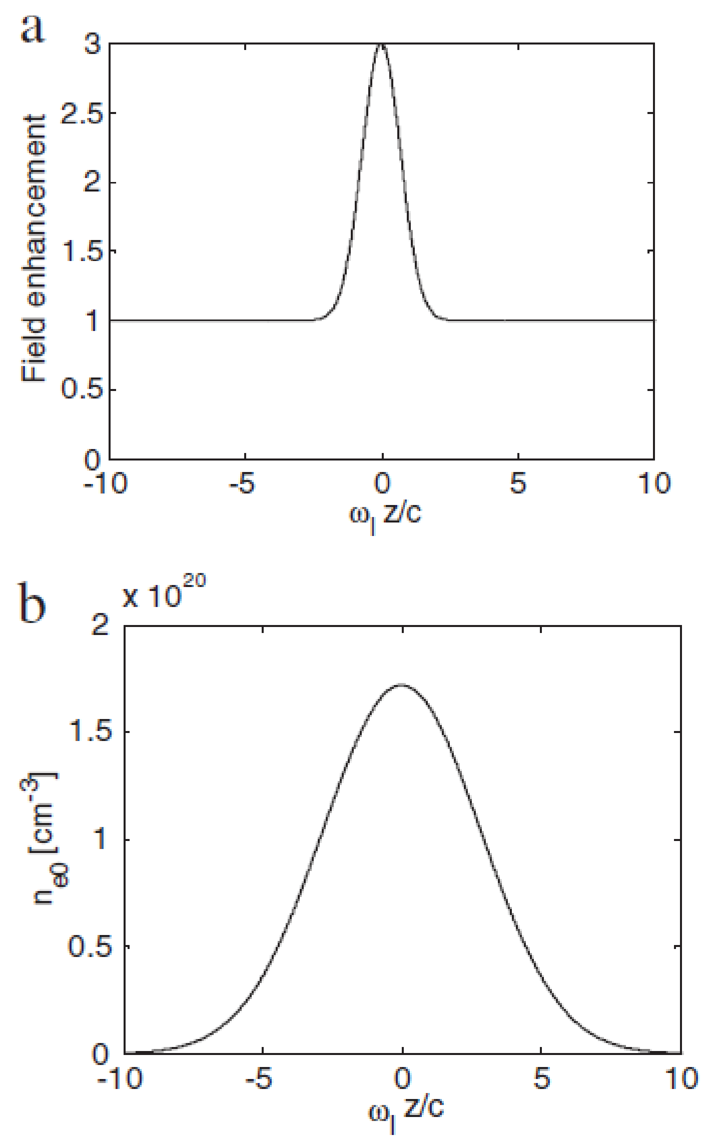

Zigler et al., PRL 106, 134801 (2011)

Electron density gradient scale length L ~(0.5-0.1) λ

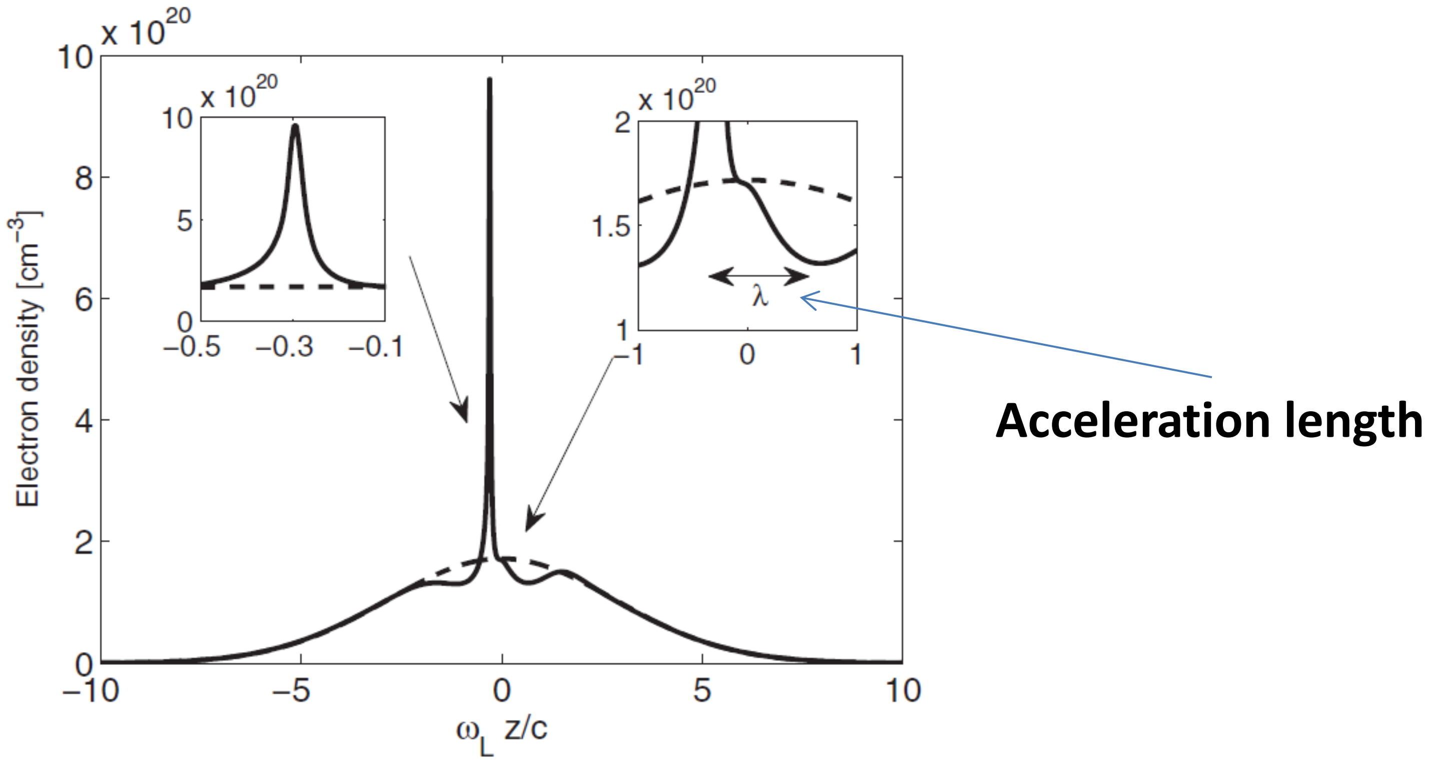

FIG. 6. Electron density normalized to the laser frequency before and after the main laser pulse has passed the frozen H_2O nanowire. Left-hand inset: Enlargement of the region of peak electron density. Right-hand inset: Enlargement of the ions' acceleration length.